NOTICE

The quality of this microform is heavily dependent upon the quality of the original thesis submitted for microfilming. Every effort has been made to ensure the highest quality of reproduction possible.

If pages are missing, contact the university which granted the degree.

Some pages may have indistinct print especially if the original pages were typed with a poor typewriter ribbon or if the university sent us an inferior photocopy.

Reproduction in full or in part of this microform is governed by the Canadian Copyright Act, R.S.C. 1970, c. C-30, and subsequent amendments.

AVIS

La qualité de cette microforme dépend grandement de la qualité de la thèse soumise au microfilmage. Nous avons tout fait pour assurer une qualité supérieure de reproduction.

S'il manque des pages, veuillez communiquer avec l'université qui a conféré le grade.

La qualité d'impression de certaines pages peut laisser à désirer, surtout si les pages originales ont été dactylographiées à l'aide d'un ruban usé ou si l'université nous a fait parvenir une photocopie de qualité inférieure.

La reproduction, même partielle, de cette microforme est soumise à la Loi canadienne sur le droit d'auteur, SRC 1970, c. C-30, et ses amendements subséquents.

ACTIVATION OF METHANE ON SUPPORTED METAL CATALYSTS

BY

Lyn M. Brimacombe, B.Sc.(Hon.)

A Thesis
Submitted to the School of Graduate Studies
in Partial Fulfilment of the Requirements
for the Degree
Masters of Science

ISBN 0-315-70523-X

UNIVERSITÉ D'OTTAWA
UNIVERSITY OF OTTAWA

TABLE OF CONTENTS

		Page
ABSTRACT		iii
ACKNOWLEDGEMENTS		iv
LIST OF FIGURES		v
LIST OF TABLES		vi
CHAPTER		
1	INTRODUCTION	1
2	EXPERIMENTAL METHODS	9
	2.1 Apparatus	9
	2.2 Materials	13
3	CHARACTERIZATION OF CATALYSTS	15
	3.1 Introduction	15
	3.2 Experimental Procedure	16
	3.3 Results and Discussion	19
	3.4 Summary	24
4	TEMPERATURE PROGRAMMED REACTIONS (TPR)	25
	4.1 Introduction	25
	4.2 Experimental Procedure	27
	4.3 Results and Discussion	28
	4.4 Summary	49

TABLE OF CONTENTS (Cont'd)

		Page
5	ISOTHERMAL REACTIONS OF METHANE ON SUPPORTED METAL CATALYSTS	51
	5.1 Introduction	51
	5.2 Experimental Procedure	52
	5.3 Results	53
	5.4 Discussion	55
	5.5 Summary	58
6	METHANE-ETHYLENE COUPLING REACTIONS	59
	6.1 Introduction	59
	6.2 Experimental Procedure	60
	6.3 Results	60
	6.4 Discussion	67
	6.5 Summary	69
7	CONCLUSIONS	70
	APPENDIX A	71
	APPENDIX B	72
	APPENDIX C	80
	REFERENCES	82

ABSTRACT

In order to obtain more information required for the catalytic conversion of methane, the interaction of methane and ethylene with various supported metal catalysts was investigated. The metals used were Ni, Fe, Co, Mo, Ru, Rh, Pd, Re, Ir, and Pt, all supported on Al_2O_3. Silica supported nickel was also used. The technique of temperature programmed reaction was mainly used. This method gives temperatures at which the adsorption and/or the reaction of a gas starts to occur. The present results showed wide differences in the interaction of methane or ethylene with each catalyst. The isothermal reaction of methane was also carried out in order to further investigate the behaviour of the CH_n species which were formed upon the chemisorption of methane.

As a process for converting methane to higher hydrocarbons, the catalytic coupling of methane with ethylene ($CH_4 + C_2H_4 \rightarrow C_3H_8$) was examined by using the catalysts listed above. At 250 and 350°C, no propane was produced on any of the catalysts, except for alumina supported platinum. A trace of propane was found in this case for the reaction at 250°C. The results were discussed based on the interaction of the reactants with these metals as revealed by the temperature programmed reactions.

ACKNOWLEGEMENTS

I would sincerely like to thank my co-supervisors, Dr. Y. Amenomiya and Dr. B.A. Morrow for their guidance and advice throughout the course of this work.

A special heartfelt thanks goes to my parents, Jack and Norma Kearns, who have always given support, love and encouragement towards everything I have done. I appreciate all the times they have gone out of their way to help me, including emergency babysitting.

Lastly, I would like to thank my husband, Bob, and son Christopher for their patience while I completed this work. I am especially grateful for Bob's help in obtaining the final versions of my thesis.

LIST OF FIGURES

FIGURE	Page
1.1 Gibb's Free Energy Change of Reactions Related to Methane Conversion	3
2.1 Schematic Diagram of Reaction System	10
2.2 Reactor	11
3.1 Hydrogen Adsorption Isotherm for 5% Ni/Al_2O_3 at 20°C	18
4.1 Methane TPR Profile for 9.6% Ni/SiO_2 and curve representing thermodynamic equilibrium	31
4.2 Methane TPR Profile for 5% Ru/Al_2O_3	34
4.3 Methane TPR Prodile for 9.5% Co/Al_2O_3	35
4.4 Ethylene TPR Profile for 5% Ni/Al_2O_3	40
4.5 Ethylene TPR Profile for 0.5% Pd/Al_2O_3	43
4.6 Ethylene TPR Profile for 1% Ir/Al_2O_3	45
4.7 Ethylene TPR Profile for 9.6% Co/Al_2O_3	48

LIST OF TABLES

TABLE	Page
1.1 Thermodynamic Calculations for the Simultaneous Processes of Complete Methane decomposition (K_1) and Ethane Formation (K_2)	7
3.1 Characterization of Catalysts	20
4.1 Characteristic Temperatures from the Methane TPR Profiles	29
4.2 Analysis of the Final Products of the Methane TPR	30
4.3 Characteristic Temperatures from the Ethylene TPR Profiles	38
4.4 Analysis of the Final Products of the Ethylene TPR	39
4.5 Comparison of Ethylene TPR for 5% Ni/Al_2O_3, 9.6% Ni/SiO_2 and 0.5% Rh/Al_2O_3	41
4.6 Final Products of Ethylene Reactions on 1% Pt/Al_2O_3	46
5.1 Results of Isothermal Methane Reactions at 500°C	54
6.1 Thermodynamic Data for the Coupling Reaction, $CH_4 + C_2H_4 \rightleftharpoons C_3H_8$	61
6.2 Results of Methane-Ethylene Coupling Reaction	62

Chapter 1

INTRODUCTION

Conversion of methane to higher hydrocarbons can be a commercially valuable process for production of chemical feedstocks and gasoline if high efficiencies and selectivities can be obtained. Given the abundance of natural gas, methane is an easily obtainable and inexpensive reactant. As a process of converting methane to higher hydrocarbons without going through syngas, oxidative coupling of methane is being widely investigated where oxygen is used in the activation of methane. The extensive work has been summarized in a recent review.[1] Oxygen and methane can either be passed simultaneously over the catalyst or cyclically (cycles of one reactant, then the other). Oxygen can diffuse as deep as 10 to 12 atomic layers into the catalyst, oxidizing the metal to higher valence states.[2] The oxidative coupling reaction via cyclic feeding can be represented in the following equations, where * indicates an adsorbed species.

$$O_2 + 2\ M^{(2n-2)+}O_{n-1} \rightleftharpoons 2\ M^{(2n)+}O_n$$

$$2\ CH_4 + 2\ M^{(2n)+}O_n \rightleftharpoons 2\ CH_3 + 2\ *OH + 2\ M^{(2n-2)+}O_{n-1}$$

$$2\ CH_3 \rightleftharpoons CH_3CH_3$$

Some of the problems that arise from this process involve competition between the coupling reaction and the complete oxidation of methane to carbon dioxide. This leads to a poor selectivity to C_2 unless the catalyst and the reaction conditions are carefully

selected. In general, the reaction is only viable at high temperatures, usually 700 to 900°C.

An alternative process of methane conversion which bypasses syngas is the coupling of methane with olefins, as in the example below.

$$CH_4 + C_2H_4 \rightarrow C_3H_8$$

The temperature dependence of the free energy change of the above reaction is compared with those of some other related reactions in Figure 1.1. As seen in Figure 1.1, the methane-ethylene coupling reaction is thermodynamically favoured at temperatures below 300°C. Therefore, the catalytic coupling of methane with olefins is expected to proceed at a much lower temperature than required for the oxidative coupling process discussed above. Further, the absence of oxygen assures that complete oxidation to CO_2 does not occur. The formation of carbon from ethylene via the reaction:

$$2\ C_2H_4 \rightarrow C + C_3H_8$$

is more favoured thermodynamically than the methane coupling with ethylene, as seen in Figure 1.1. Therefore, the selectivity of the catalyst will be an important consideration. Finally, although a reaction temperature below 300°C is favoured, it will also be important that a suitable catalyst have sufficient kinetic activity at such low temperatures in order to be of practical use.

Liquid superacids have been used with success to catalyze the methane-ethylene coupling reaction.[3,4] Pressurized systems were a required condition. Olah *et al.*[5] studied

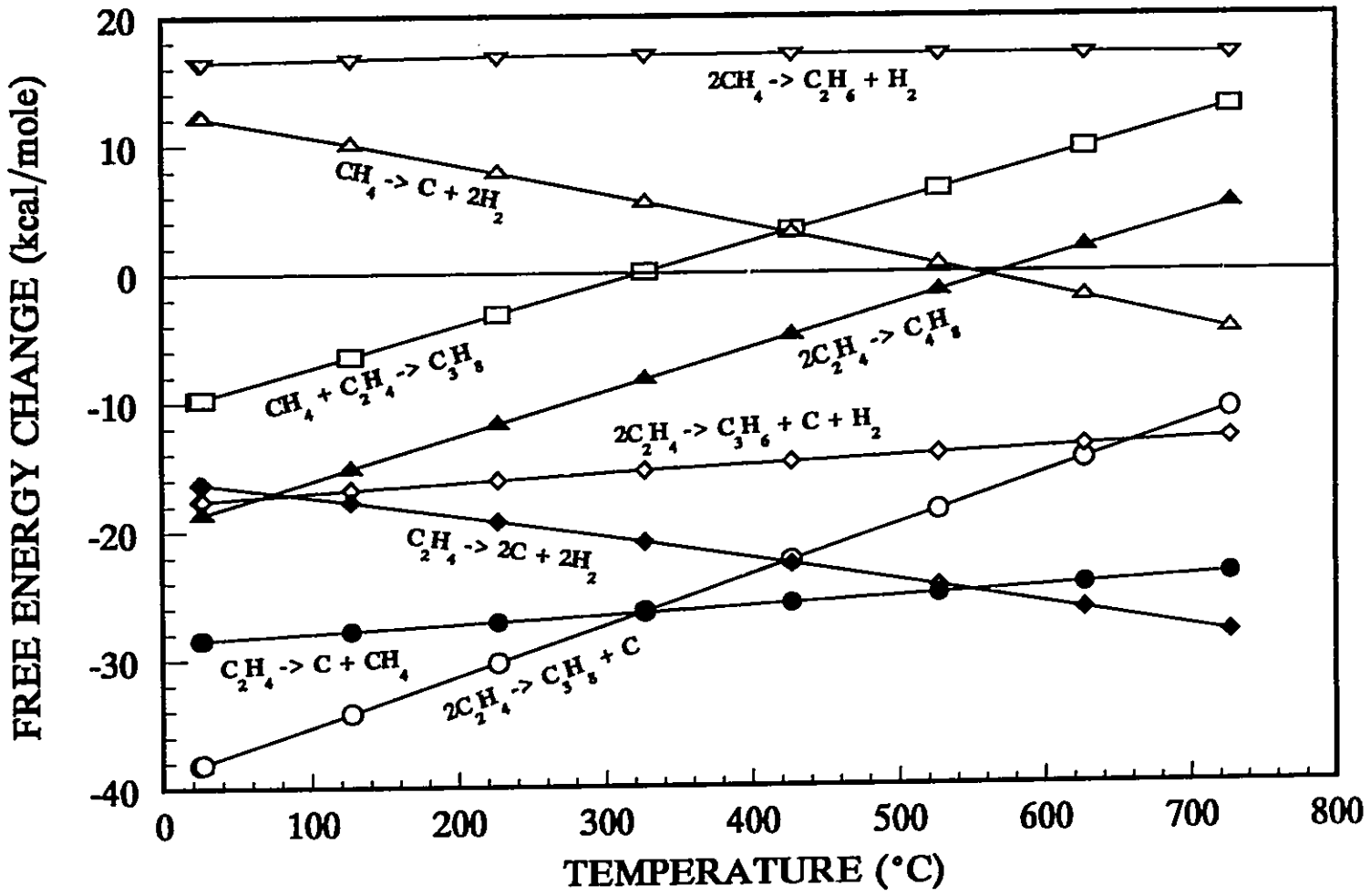

Figure 1.1 Gibb's free energy change of reactions related to CH_4 conversion.

solid superacids (SbF_3 intercalated in graphite, TaF_3 on AlF_3 and TaF_5). Using $^{13}CH_4$ labelling, Olah and coworkers could distinguish between methane-ethylene coupling and ethylene self-condensation cracking reactions. Propane was produced from methane-ethylene coupling over TaF_5 at 14.1% and over SbF_5/graphite at 30.2% of the ethylene reactant concentration. The $^{13}CH_4/C_2H_4$ ratio was 110/1. Olah found that when the ethylene concentration exceeded 1 mole %, the ethylene self-condensation cracking process became predominant in the formation of propane. At ethylene concentrations of 8 mole %, the ethylene self-condensation cracking process was responsible for production of all the propane.

Olah has proposed the following mechanism for the coupling reaction in the presence of a superacid.[5]

$$CH_2CH_2 \overset{H^+}{\rightleftharpoons} CH_3CH_2^+ \overset{^{13}CH_4}{\rightleftharpoons} \left[CH_3CH_2 \text{---} \overset{H}{\underset{^{13}CH_3}{<}} \right] \rightarrow CH_3CH_2{}^{13}CH_3$$

The reaction is acid catalysed and an ethyl cation is formed upon protonation of ethylene. The cation forms a pentacoordinate intermediate with methane, producing propane.

Coupling has also been observed by Scurrell[6] using a sulphate treated zirconia as a solid superacid catalyst (P = 19 atm, CH_4/C_2H_4 = 2 to 3). Large quantities of C_6 and C_7 hydrocarbons were produced. Actual methane-ethylene coupling and oligomerization reactions could not be differentiated in the study, though Scurrell believed that oligomerization occured to a large extent. Further studies need to be done using this

catalyst before it can be definitely said that methane-ethylene coupling can occur.

The coupling of methane with olefins on supported-metal catalysts has also been reported.[7,8] This is an interesting and useful route to the coupling reaction because of the ease of catalyst preparation and handling. However, the mechanism of the reaction is not clear and selectivity is still low. Therefore, more information is needed before the methane-ethylene coupling reaction can become commercially practical.

As decribed so far, there are various processes for converting methane to higher hydrocarbons. In any process, however, the activation of methane is the first step required for conversion. Methane is generally known to have a very low reactivity. The CH bond strength of methane for removal of the first hydrogen is 103 kcal/mole which is much greater than the metal-hydrogen bond strengths. Therefore, for methane to adsorb on a metal surface, the metal atom must insert into the CH bond by oxidative addition.[9] Methane activation energies for adsorption have been determined to be 7[10] and 6[11] kcal/mole for Ni/SiO_2. Ni(111) surfaces were found to have adsorption activation energies of 12 and 13 kcal/mole while Ni(100) had lower activation energies of 6 and 9 kcal/mole.[12] Similar activation energies were calculated or determined for other metals such as 10[9] and 11[13] kcal/mole for Pt(111), 8 kcal/mole for Fe(100)[9] and 7 kcal/mole for Rh.[14]

Methane adsorption on supported metal catalysts has been observed to occur at room temperature,[10,11,15-17] though only to a small extent. Dissociative adsorption is believed to occur either partially or completely leading to carburization of the catalyst.

IR studies of methane adsorption on Ni/SiO_2 were attempted by Erkelens and Wosten[18] but they were unable to observe any CH_n absorption bands at temperatures up to 100°C. They felt that the reason CH_n species were not detected was due to the small

quantities of partially dissociated species that may have been present on the catalyst surface rather than there not being any of these species present. Kuijpers and coworkers also studied adsorption of CH_4 on Ni/SiO_2 using IR spectroscopy.[16] They could not detect any CH_n species on the catalyst surface either, although when using NMR, evidence of adsorbed partially dissociated methane was found. They argued that methane dissociated to carbon and hydrogen initially on the catalyst surface and the deposit caused more close packing of the metal crystallographic planes. Additional CH_4 was then believed to adsorb with partial dissociation.

Studying the activation of methane in a catalytic environment is an important step in finding a viable way to convert methane to more desirable higher hydrocarbons. Methane has very low reactivity and does not adsorb as strongly as other hydrocarbons on many catalysts. The aim of this Thesis has been to investigate the interaction of methane with various supported group 8 metal catalysts. Temperature programmed reaction (TPR) was mainly used for this purpose. This technique not only shows temperatures at which the adsorption, desorption and reaction occur, but also gives indications of the type of reactions and the surface residue. The TPR of ethylene was also included for comparison.

In order to investigate the decomposition of methane and the possible formation of ethane from methane, isothermal reactions of methane on the catalysts were studied at temperatures of 250 and 500°C. The turnover frequencies (TOF) were determined for ethane formation and surface carbon formation.

As stated earlier, dissociative adsorption of methane on metal catalysts is believed to occur[10,16] when methane comes in contact with a catalyst surface. The ethane formation reaction ($2\ CH_4 \rightleftharpoons C_2H_6 + H_2$) must compete with the reaction of complete dissociation

of methane to carbon and gaseous hydrogen. Table 1.1 shows results from thermodynamic calculations of the simultaneous process of complete methane dissociation (K_1) and ethane formation (K_2) at a range of temperatures. Formation of ethane is thermodynamically possible under the conditions outlined in Table 1.1, but the expected quantity of ethane that is produced is very small. The production of hydrogen in K_1 causes the reaction in K_2 to go to the left, resulting in less ethane formation:

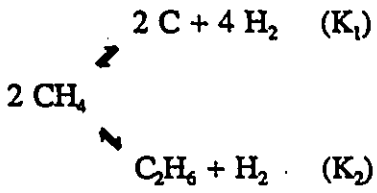

Table 1.1 Thermodynamic Calculations for the Simultaneous Processes of Complete Methane Decomposition (K_1) and Ethane Formation (K_2).

TEMP (°C)	K_1	K_2	CONVERSION % TO SURFACE CARBON	CONVERSION % TO ETHANE
250	$8.80X10^{-4}$	$8.76X10^{-8}$	12.41	$5.0X10^{-5}$
300	$4.54X10^{-3}$	$3.43X10^{-7}$	25.94	$7.0X10^{-5}$
350	$1.84X10^{-2}$	$1.10X10^{-6}$	44.98	$7.0X10^{-5}$
400	$6.18X10^{-2}$	$2.99X10^{-6}$	65.41	$5.0X10^{-5}$
450	$1.77X10^{-1}$	$7.15X10^{-6}$	81.34	$3.0X10^{-5}$
500	$4.47X10^{-1}$	$1.53X10^{-5}$	90.79	$1.0X10^{-5}$

The free energy changes of reaction over a wide temperature range for methane can be observed in Figure 1.1. Entropy works in favour of the reaction $CH_4 \rightleftharpoons C + 2\ H_2$ with increasing temperatures, whereas for the reaction $2\ CH_4 \rightleftharpoons C_2H_6 + H_2$, the entropy only slightly inhibits the reaction with increasing temperature. Therefore, thermodynamically, lower reaction temperatures would be expected to give slightly higher yields of C_2H_6. This would also be expected to decrease the extent of methane dissociation.

Finally, experiments were carried out to investigate the methane-ethylene coupling reactions. The results obtained from the TPR experiments gave some insight into the behaviour of the reactants at different temperatures. Evidence of coupling would be of interest since higher hydrocarbons are more commercially valuable as chemical feedstocks or fuels.

A closed recirculation reaction system directly connected to a gas chromatograph was used for all the experiments carried out in this work. The catalysts that were used in the experiments were characterized by determining the number of metal active sites, dispersion factors and surface areas.

Chapter 2

EXPERIMENTAL METHODS

2.1 APPARATUS

All of the experimental results presented in this thesis were obtained using the apparatus shown schematically in Figure 2.1. It is a closed, greaseless recirculation reaction system which is directly connected to a gas chromatograph.

The research grade gases (O_2, C_2H_4, CH_4, H_2, C_2H_2, N_2) were introduced through valves 8 to 11. Valves 1 to 11 are all bellows sealed metal valves. Copper tubing was used to connect the valves to valve 7. The rest of the tubing in the system was either stainless steel or pyrex. Valve 6 opens the system to the vacuum manifold consisting of a rotary pump (Vac Torr, model 25) and a 1 inch oil diffusion pump (Edwards Speedivac). A thermocouple vacuum gauge (Type GTC - 100) and a cold-emission ionization gauge both from Consolidated Vacuum Corporation were used to measure the pressure in the manifold. Valve 5 introduces the gases to the reaction circulation system. The volume contained by valve 5, 4, 2 and 12 will be referred to as volume V_1 (Dead Volume = 38.175 cm^3). The volume contained by valve 4 and 3 will be referred to as volume V_2 (Dead Volume = 9.956 cm^3). The amounts of reactant gases were measured manometrically in volumes V_1 and V_2 before mixing by circulation. The reactor was made out of quartz and its volume is taken as the volume contained by valve 1 and 2. To ensure that the system was as leak-free as possible, the reactor was cut out to change the catalyst and glass blown in place again. Figure 2.2 shows the reactor. A thermocouple jacket ran down inside the reactor so the tip of the thermocouple wire was

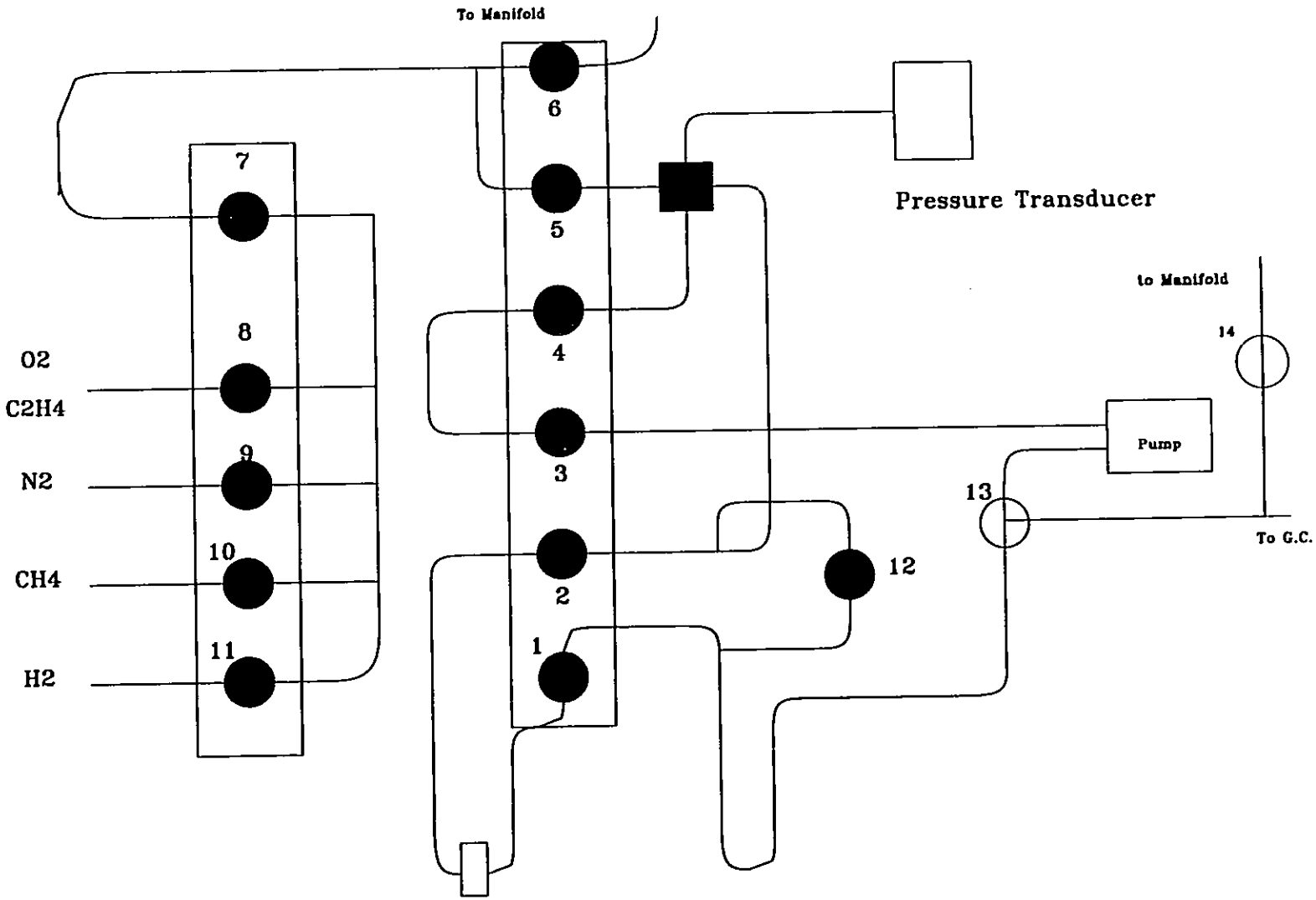

Figure 2.1 Schematic Diagram of Reaction System

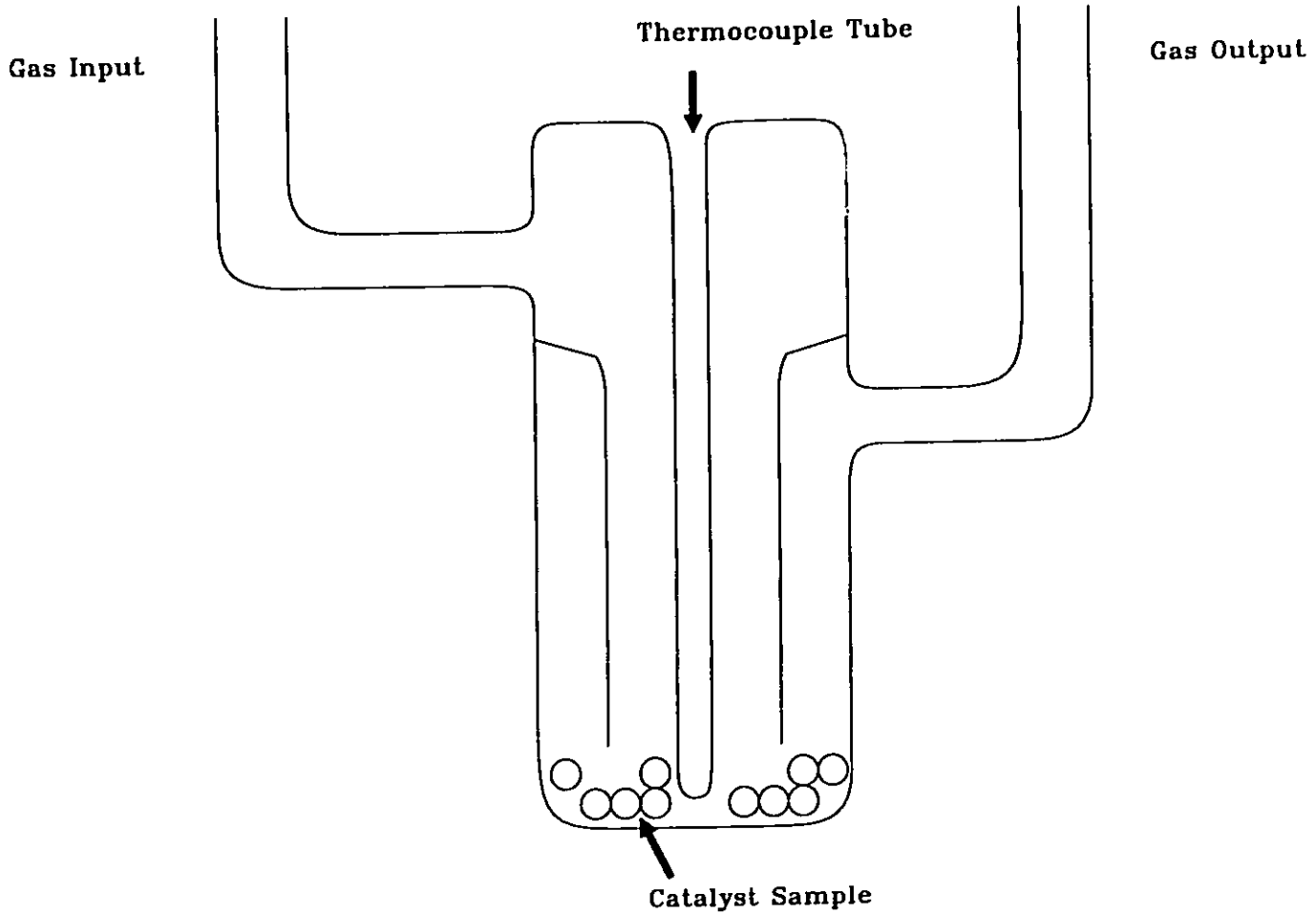

Figure 2.2 Reactor

buried in the catalyst bed. A type K thermocouple was used to monitor the catalyst temperature. The reactor was heated with a block furnace controlled either by a digital Athena temperature controller or by an analog temperature programmer (Theall Eng. Co.) for experiments where the catalyst temperature was increased with time. When the temperature programmer was used, a two pen recorder monitored the response of temperature and pressure.

The reactor was filled with catalyst up to approximately a quarter inch from the inner tube surrounding the thermocouple jacket. The reactant gas was passed through valve 2 to the inner tube, circulated over the catalyst to the outer tube and exited at valve 1. The gas was continually circulated by closing the bypass valve 12. Valve 13 was a 3-way valve and was closed to a 2-way passage. The reactant gas circulated through a bellows circulation pump model MB-21 manufactured by the Metal Bellows Company. The volume contained by valve 1, 12 and 3 will be referred to as volume V_C. After passing through volume V_1 and V_2, the reactant gas returned to the reactor. A capacitance manometer (MKS Baratron) measured the pressure in the vicinity of V_1.

A Varian Model 3700 gas chromatograph was on line to the system when valve 13 was opened to 3-way. The volume between valve 13 and the gas sampling valve can be evacuated by opening valve 14 to the manifold. The pressure of the volume contained by valve 13, 14 and the gas sampling valve was monitored by the thermocouple gauge. The gas sample was collected in a sample loop and was then injected into the helium carrier gas stream (flow rate: 13.3 cm^3/min). The column (3.2m) was n-octane/porasil C (Durapak) and was operated at 50°C. The sample was first analysed by a thermal conductivity detector (TCD) heated to 100°C. From the TCD, the sample entered a column of porasil B (0.8m) also heated to 50°C, leading to a flame ionization detector

(FID). A Spectra-Physics SP4290 integrator was used to integrate the TCD response while a Hewlett Packard 3390A integrator was used for the integration of the FID signal.

2.2 MATERIALS

The supports used in preparing the catalysts were Alon γ-alumina from Cabot Corporation, or fumed σ-silica from Sigma Chemical Company. Alumina (particle size: 0.03 μm) and silica (particle size: 0.007 μm) had BET surface areas of 100 m^2/g and 400 m^2/g respectively.

Air (breathing quality), H_2 (UHP, 99.995%) and He (UHP, 99.999%) gases were supplied by Air Products. Matheson supplied CH_4 (UHP, 99.97%), C_2H_2 (Purified, 99.97%), O_2 (99.6%) and C_2H_4 (C.P., 99.5%) reactant gases.

2.2.1 Catalysts

5.0% Ni/Al_20_3 (Preparation by Coprecipitation): The catalyst was prepared by dissolving $Ni(NO_3)_2 \cdot 6H_2O$ (2.5g) in demineralized water (300 ml). Alumina (9.5g) was added to the solution while stirring. The mixture was heated to 80°C with continued stirring. The nickel was precipitated by slowly adding Na_2CO_3 (0.25 mole/l, 25 ml) to the alumina suspended $Ni(NO_3)_2$ solution for a period of 1 hour. The mixture was then stirred for an additional hour at 80°C. The precipitate was filtered and washed with demineralized water. The catalyst was dried at 110°C for 2 hours and calcined at 400°C for 2 hours. After crushing in a mortar, the catalyst was sieved to collect a range of 16 to 32 mesh size.

9.6% $Ni/Si0_2$ (Preparation by Impregnation): Preparation of the catalyst was carried out by dissolving $Ni(NO_3)_2 \cdot 6H_2O$ (5 g) in demineralized water (344 ml). Silica (9.5 g)

was added to the stirred solution and the mixture was heated on a hot plate with continued stirring until all of the water had evaporated. The catalyst was dried in an oven at 100°C for 2 hours. The crushing of the catalyst was carried out in the same manner as above.

9.5% Co/Al_2O_3: The catalyst was prepared by impregnation in the same manner as for 9.6% Ni/SiO_2 except $Co(NO_3)_2 \cdot 6H_2O$ (5 g) was the precursor ion and alumina (9.5 g) was used as the support.

10.0% Fe/Al_2O_3 (Preparation by Impregnation): $Fe(NO_3)_3 \cdot 9H_2O$ (7.2g) was dissolved in demineralized water (359 ml) and alumina (9 g) was slowly added to the stirred solution. The catalyst was prepared following the same procedure as that for 9.6% Ni/SiO_2.

2.3.2 Commercial Catalysts

The commercial catalysts 0.5% Rh, 0.5% Pd, 1% Pt, 1% Ir and 0.5% Ru supported on 1/8" alumina pellets were supplied by Engelhard Corp. The BET surface areas were quoted as 90 m^2/g. The Re catalyst was purchased from Aldrich and was supported on 1/8" alumina pellets. Strem Chemicals supplied the 10 to 12% Mo_2O_3 catalyst also supported on 1/8" alumina pellets (BET surface area: 64 m^2/g).

Chapter 3

CHARACTERIZATION OF CATALYSTS

3.1 INTRODUCTION

The catalysts were characterized by determining the number of surface metal sites, dispersion factors and surface areas. Catalysts of various loadings were compared on a per surface metal site basis.

Surface areas were determined using the Brunauer, Emmett and Teller (BET) method by manometric means. The number of surface metal sites were determined from hydrogen adsorption studies. H_2 adsorption becomes totally reversible at approximately 525 K.[19] The amount of reversibly adsorbed H_2 depends on temperature and metal crystallite size.[20] Bartholomew and Pannell found that at room temperature 40% of H_2 was reversibly adsorbed on Ni/Al_2O_3 with a 14% loading.[21]

The ratio of adsorbed H_2 to surface metal sites has been investigated by many groups.[21-23] It was found in all cases that H_2 adsorbed dissociatively so that the ratio of H/Ni site was 1. Techniques such as x-ray line broadening, hydrogen chemisorption, transmission electron microscopy and magnetic studies were used in these studies. Bartholomew and Pannell showed that the H/Ni site ratio stayed at 1 over various loadings and dispersions of metal.[21] Therefore, the number of metal sites exposed on the surface can be calculated from the amount of hydrogen which saturates the surface in a monolayer. Alumina and silica supports were found to show negligible adsorption of H_2 at 25°C, so that no correction for adsorption by the support need be made for H_2 adsorption studies at room temperature.

Hydrogen adsorption on metal oxides is negligible compared to the reduced metal. Therefore, the number of metal sites measured by hydrogen adsorption essentially pertains to those sites that are reduced.[21,24,25] Kuijpers and coworkers specifically investigated H_2 adsorption on NiO at 30°C and also found no adsorption.[26] For noble metals it can be assumed that all surface metal sites are easily reduced, although for base metals this may not be the case. Base metal oxides have strong interactions with alumina and silica supports and may be very difficult to reduce.[21] This may cause some error in the determination of metal dispersion.

3.2 EXPERIMENTAL PROCEDURE

3.2.1 Reactor Volume

The reactor volume, V_R, was determined for each catalyst sample. A room temperature water bath was placed around the catalyst in the reactor. Helium was admitted into V_1 and this volume of gas was expanded into V_R. The system was evacuated and the process was repeated in triplicate. The volume of the reactor was determined from the expansion of a known volume to the reactor.

3.2.2 Pretreatment of Catalysts

All catalysts were pretreated under flowing hydrogen at 80 cm^3/min. The flow rate was controlled by a multiple mass flow controller (Matheson model 8249). The high flow rate was used to ensure quick removal of water from the catalyst upon reduction. The temperature was increased at 5°C/min from room temperature. The reduction was continued at 400°C to a total reduction time of 8 hrs. Prior to each experiment, the

catalyst was further reduced at 400°C for 1 hr in circulating hydrogen and then evacuated at 400°C for 30 min.

3.2.3 BET Surface Area Measurement

Volume V_1 of the system was opened to the atmosphere and the atmospheric pressure was recorded. The freshly reduced catalyst was evacuated at 400°C for 30 min and then cooled to -196°C. Nitrogen gas was admitted into V_1. After a pressure reading was recorded for V_1, the gas was expanded to the reactor. When the adsorption reached equilibrium, the pressure reading (P) was recorded. Additional nitrogen gas was then admitted into V_1 and the same procedure was followed as initially. Nitrogen gas additions were continued until the relative pressure, P/P^o, (P^o = vapour pressure) reached about 0.35. The surface area was calculated from the saturated amount of monolayer which was determined from the BET plot.

3.2.4 Hydrogen Adsorption Measurement

Freshly reduced catalyst was evacuated at 400°C for 30 min. A water bath at room temperature was placed around the reactor and was allowed to equilibrate. The same procedure as for the BET surface area measurements was followed for measuring the adsorbed amounts of hydrogen. The procedure was continued until the equilibrated pressure reached about 160 torr. A plot of the number of moles of H_2 adsorbed versus pressure gave a y-intercept by extrapolation of the linear portion at high pressures as shown in Figure 3.1. The y-intercept represented the total number of moles of H_2 (X) which saturated the metal sites on the catalyst surface in a monolayer. Metal dispersions were calculated as $\%D = (2X)/M \times 100$, where M represents the total number of moles

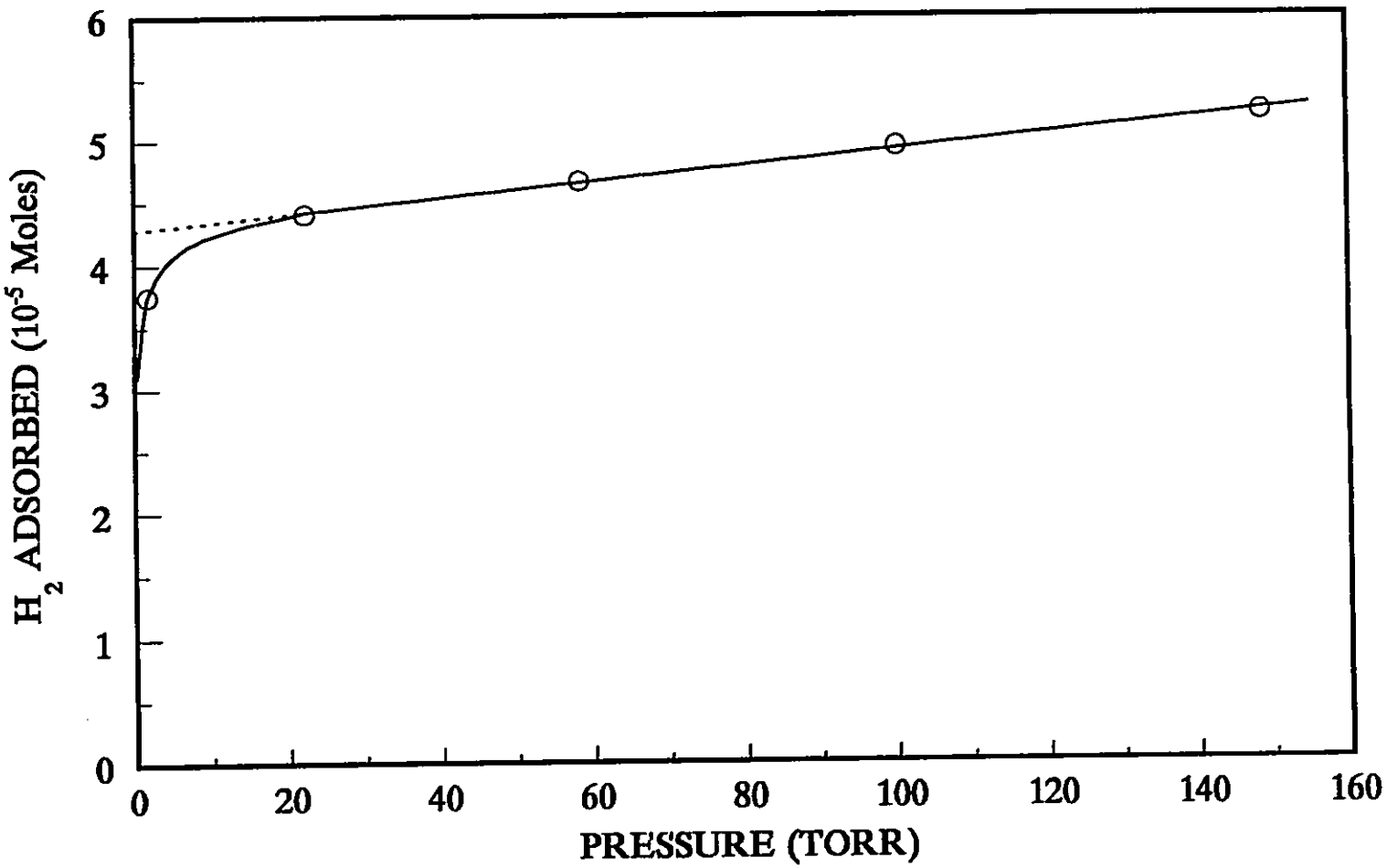

Figure 3.1 Hydrogen adsorption isotherm for 5% Ni/Al_2O_3 at 20° C.

of metal atoms calculated from the metal loading and the amount of catalyst in the reactor.

3.3 RESULTS AND DISCUSSION

The metal dispersions and the surface areas measured are listed in Table 3.1. The catalysts that were prepared for this study had higher metal loadings than the purchased commercial catalysts. The lower limit of detection of metal sites on the catalyst in the reactor was in the range of 10^{-7} moles/catalyst charge. The prepared catalysts had numbers of metal sites well above this limit while the commercial catalysts had lower numbers of metal sites which in some cases were close to the detection limit. In one case, that of 0.5% Re/Al_2O_3, the number of surface sites could not be accurately calculated experimentally due to the detection limit of the experiment. For future experiments, a larger reactor is planned that will accommodate a larger sample size and therefore this will improve the detection limit.

In the initial reduction of the freshly prepared catalysts, a heating rate of 5°C/min was used to allow the reduction process to proceed slowly and under control. This was to inhibit, as much as possible, any sintering occurring due to the contact of water with the crystallites. It has been found that the presence of water can cause aggregation of the crystallite particles.[27,28] For the precalcined 5% Ni/Al_2O_3 catalyst, water is produced by the reduction process:

$$NiO + H_2 \rightarrow Ni + H_2O \qquad \Delta H°(25°C) = 0.4 \text{ kcal/mole}$$

By heating the catalyst more slowly, the rate of formation of water is slower and the

Table 3.1 Characterization of Catalysts

CATALYST	MASS OF CATALYST (g)	SURFACE METAL SITES (moles/g)	DISPERSION FACTOR (%)	BET SURFACE AREA (m^2/g)
Ni/Al_2O_3[a,b]	0.4573	3.521×10^{-5}	4.1	
Ni/SiO_2[b,c]	0.3142	1.567×10^{-5}	1.8	
Ni/SiO_2[c,d]	0.4357	3.279×10^{-4}	8.2	
	0.1388	2.100×10^{-5}	9.2	
Mo/Al_2O_3[b]	0.6588	6.851×10^{-5}	5.5to6.6	
Co/Al_2O_3[c]	0.5345	3.391×10^{-5}	2.1	138
	0.2146	4.812×10^{-5}	3.0	
Fe/Al_2O_3[c]	0.3965	6.366×10^{-6}	0.4	290
Ru/Al_2O_3	0.4361	1.510×10^{-6}	3.1	
Pt/Al_2O_3	1.0542	1.773×10^{-5}	34.8	
Rh/Al_2O_3	0.4836	8.511×10^{-6}	17.5	
Re/Al_2O_3	0.4023			322
Pd/Al_2O_3	0.5225	1.448×10^{-5}	30.8	255
Ir/Al_2O_3	0.4563	1.885×10^{-5}	36.2	

[a] precipitated
[b] calcined
[c] impregnated
[d] relates to the 9.6% w/w catalyst

hydrogen stream can more efficiently remove the water before extensive contact with the surface occurs.

For the catalysts that were not calcined, additional water can be produced during the reduction. Taking the nickel catalyst as an example, $Ni(NO_3)_2 \cdot 6H_2O$ has not been decomposed and all the water from the impregnation process was not likely removed when dried at 100°C. The decomposition of $Ni(NO_3)_2$ can occur in the following ways:

		ΔH° (25°C) (kcal/mole)
1)	$2\ H_2 + Ni(NO_3)_2 \rightarrow Ni + 2\ H_2O + 2\ NO_2$	11.9
2)	$4\ H_2 + Ni(NO_3)_2 \rightarrow Ni + 4\ H_2O + 2\ NO$	-86.5
3)	$9\ H_2 + Ni(NO_3)_2 \rightarrow Ni + 6\ H_2O + 2\ NH_3$	-261.2

Bartholomew and Farrauto have observed the presence of NO and NO_2, especially in the range of 220 to 250°C,[25] verifying that these decomposition processes do occur. Reaction 2 and 3 are very exothermic and sintering may follow due to overheating. The slow heating rate of 5°C/min used also minimized overheating.

During the reduction process, high flow rates of hydrogen (80 cm^3/min) were used to drive off the water as quickly as possible and to aid in heat transfer during decomposition of $Ni(NO_3)_2 \cdot 6H_2O$. A flow rate of 40 cm^3/min was used initially but some condensation was observed on the reactor. Therefore, the flow rate was increased to 80 cm^3/min and the water was assumed to be removed efficiently enough to inhibit interaction of water with the surface.

The 5% Ni/Al_2O_3 catalyst, which was prepared by coprecipitation and calcination, was

found to have a dispersion of 4.1%. The dispersion of a 5% Ni/SiO_2 catalyst (not listed in Table 3.1) prepared in the same manner could not be determined because the quantity of adsorbed H_2 was too small to be accurately measured (adsorption in the range of 10^{-8} - 10^{-7} moles H_2/catalyst charge). To determine if the small quantity of surface metal sites was due to low dispersion or to a large fraction of unreduced nickel, the per cent reduction of the Ni metal was investigated by the oxidation of the reduced catalyst with oxygen at 550°C. The oxidized nickel was assumed to be NiO since Ni_2O_3 and NiO_2 are not stable under anhydrous conditions.[29] Also, nickel catalysts with metal loadings above 5% were found by other workers to be in the form of NiO.[30] The oxidation experiment revealed that all the nickel was reduced to nickel metal under the present reduction conditions. Therefore, low dispersion was responsible for the small quantity of surface nickel. To increase the number of surface metal sites on the catalyst, the metal loading was doubled in preparing a new Ni/SiO_2 catalyst. Bartholomew and Farrauto found that increasing the metal loading had an effect of increasing surface metal sites up to 25 wt%, after which it remained relatively constant.[25] By increasing the metal loading in this case, the dispersion would probably be decreased further. However, other techniques (ie. method of pretreatment) as discussed earlier were used in the hopes of having a positive effect on increasing the total number of exposed metal atoms.

Impregnation techniques were used for further preparations of catalysts rather than coprecipitation. It has been found that under similar conditions, catalysts prepared by impregnation yield higher dispersions than those prepared by coprecipitation.[25]

In the present study, calcination has been found to have a negative effect on dispersion. It is believed that sintering occurs during calcination. The effect of lowering dispersion by calcination has been noted by various workers.[27,28]

A hydrogen adsorption study of 5% Ni/SiO_2 (impregnated, calcined) revealed a dispersion of 1.8% which was relatively low, although for the 5% Ni/SiO_2 (coprecipitated, calcined), the quantity of surface metal sites was below the detection limit of the experiment. Under these circumstances, the impregnation method of preparation gave a higher dispersion compared to the coprecipitation method. Therefore, the preceeding catalysts were prepared by the impregnation technique. The 9.6% Ni/SiO_2 (impregnated, uncalcined) containing double the metal loading gave a much improved dispersion factor of 8.2%. The number of surface metal sites was an order of magnitude larger than the other nickel catalysts.

The iron, cobalt and molybdenum catalysts had metal loadings which were similar to the other catalysts but showed much lower dispersion. For instance, the Fe/Al_2O_3 catalyst with a metal loading of 10% showed a very low dispersion of 0.4%. It is thought that some of the iron was present as an oxide. The iron oxide may have had strong interactions with the alumina support making it very difficult to reduce at the temperature of 400°C which was used under these circumstances. This was also believed to be the case to some extent for Co/Al_2O_3, having a dispersion factor of 2 to 3%. Galuszka and Sawicki found similar results with oxide supported iron catalysts showing dispersions up to 0.9%.[31] Bartholomew and Pannell discovered that with base metal oxides there are oxide-support interactions which interfere with the reduction of the metal to its metallic state.[21] This has been noted by others as well.[32,33] Rameswaran and Bartholomew found that the extent of reduction was exceptionally low for Fe/Al_2O_3.[33] They proposed from their results that the low reduction may be caused by the alumina being dissolved during calcination in the acidic environment of the nitrate impregnated catalyst. The dissolved alumina is then thought to partially coat some of the metal particles. Also they suggested

that iron oxide phases may have formed during preparation which would further lower the extent of reduction. Galuszka and Sawicki have presented a model of an oxide-supported iron particle which has various layers of iron oxides with very little of the iron in the metallic state.[31] The iron metal is believed not to be in contact with the oxide support.

Molybdenum as a transition metal has different properties than the other metals studied. The Mo_2O_3/Al_2O_3 catalyst was obtained commercially and then treated under reduction conditions. The catalyst was precalcined and this could have resulted in the lower dispersion compared to the 9.6% Ni/SiO_2. It was also not known if all the Mo had been reduced to the metal. The Rh, Pd, Ir, Pt, and Re dispersion range was 17 to 30% which was much higher than the dispersions for catalysts with metal loadings of 5% or greater. This was expected since higher metal loadings give lower dispersions.

3.4 SUMMARY

The way in which the catalysts were prepared and conditioned had an effect on both the number of surface metal sites and on the dispersion. With increased metal loading the number of surface metal sites per gram increased for loadings between 0.5 and 10%. The dispersion showed a general decrease with increased metal loading which is believed to be due to larger crystallite formation in catalysts with higher metal loadings.

Precalcined catalysts showed lower dispersions than the catalysts whose metal precursors were decomposed under hydrogen flow. Sintering of precalcined catalysts appeared to be at least partially responsible for lower dispersions. Also, catalysts prepared by impregnation gave higher dispersions than the coprecipitated catalysts.

Chapter 4

TEMPERATURE PROGRAMMED REACTIONS (TPR)

4.1 INTRODUCTION

Methane and ethylene chemisorption has been previously studied on various group 8 metals using techniques such as temperature programmed desorption (TPD), IR spectroscopy, electron energy loss spectroscopy (EELS), low energy electron diffraction (LEED) and nuclear magnetic resonance (NMR). Various surface species have been proposed on supported metal catalysts and on single crystals. It has been found that in some cases, the surface species on a single crystal metal can give an insight into some of the surface species found on the supported metal, although this is not the case for the adsorption of ethylene on Ni/Al_2O_3.[9]

While methane adsorbs on many metal surfaces dissociatively, as decribed in Chapter 1, the adsorption of ethylene is more complex. In the chemisorption of ethylene on some single crystal and supported metals, the ethylidyne (CCH_3) species has been predominantly observed. Steininger *et al.*[34] have detected the ethylidyne species on Pt(111) and Hatzikos *et al.*[35] have seen the same species on Pt(100) using EELS. The ethylidyne species has been found on Pt/Al_2O_3 using IR spectroscopy[36] and NMR.[37] Rh(111),[38-41] Rh/Al_2O_3,[36] Ru(0001),[42] Ru/Al_2O_3,[36] Pd(100),[43] Pd(111),[43] and Pd/Al_2O_3[44,45] showed the presence of the same major species. Beebe and Yates used IR spectroscopy to observe the presence of other minor species.[36]

In IR studies of ethylene on Ni/Al_2O_3, Lapinski and Ekerdt[46] observed adsorbed ethylidyne. A peak in the spectrum was found that may have been produced by an

adsorbed acetylene-type species, but this was not conclusive. The ethylidyne species was observed at temperatures as low as -45°C. Their study ruled out the presence of other possible species such as molecularly adsorbed C_2H_4, vinyl species and di-sigma-bonded C_2H_4. It is most probable that ethylidyne is the major species formed upon adsorption of C_2H_4 on the catalyst surface and very little CH_4 is expected to be produced from C_2H_4 decomposition at lower temperatures.[47]

Two possible mechanisms have been proposed for the formation of ethylidyne on these metals. In the first mechanism the ethylene molecule chemisorbs to two metals in a di-sigma-bond configuration. Dehydrogenation occurs on carbon, forming a vinyl ($CHCH_2$) and vinylidene (CCH_2) species. Upon hydrogenation, ethylidyne is formed.[48,49] In the second mechanism, ethylene is pi-bonded to a metal. After hydrogen insertion, a sigma-bonded ethyl (CH_2CH_3) species is formed. Adsorbed ethylidene and ethylidyne are produced after dehydrogenation at the alpha carbon.[46]

There are various factors which will help form the ethylidyne species on the surface.[46] Adsorbed hydrogen available on the surface may allow both ethylene hydrogenation and ethylidyne formation to occur. Some hydrogen may be present before ethylene adsorption or hydrogen may be made available by initial dehydrogenation of ethylene upon adsorption. Various studies of these metals have supported the presence of hydrogen produced by ethylene dehydrogenation.[50-52] The other possibility that may aid in the formation of ethylidyne is that the adsorbed intermediates may block metal sites so ethylene decomposition is less probable, thereby improving the stability of ethylidyne.

This study used temperature programmed reaction (increasing the catalyst temperature while monitoring the pressure change when the catalyst is in contact with a given reactant gas) in order to determine the interaction profile of methane and ethylene with various

supported metal catalysts. This technique is abbreviated as TPR. Special interest was focussed on temperatures where adsorption and decomposition were first detected, as well as on the final products obtained after the TPR was stopped.

4.2 EXPERIMENTAL PROCEDURE

Each catalyst was freshly reduced at 400°C for 1 hr and evacuated for 30 min at 400°C. The catalyst sample sizes were, on average, 0.5 g. After cooling to room temperature the reactant gas was admitted into volume V_1, V_2, V_C and V_R and circulated through the reactor (methane pressure: 7 torr, ethylene pressure: 17 torr). The temperature of the catalyst was increased at 8°C/min to 500°C. Pressure and temperature were recorded using a two pen recorder. Because the adsorption and decomposition of the hydrocarbons cause a decrease and increase in the pressure of the system respectively, the pressure-time curve of the TPR shows the changes in the system as a function of temperature.

To correct for increase in pressure due to thermal expansion, a helium TPR curve was obtained for each catalyst. Minimal error may occur when correcting for thermal expansion due to differences in thermal conductivity of helium compared to methane and ethylene. Correction for thermal expansion was then accomplished by comparing the helium curve to the reactant curve. The final products from the TPR were determined using G.C. analysis. The amount of H_2 in the final products was estimated by subtracting the partial pressures of the products detected by the G.C. from the final pressure in the reactor system measured by the manometer. Methane and ethylene TPR curves of the Al_2O_3 and SiO_2 supports were compared with those of the catalysts.

4.3 RESULTS AND DISCUSSION

4.3.1 Methane TPR Analysis

The catalysts were grouped according to similarities in their methane and ethylene TPR curves. Typical curves obtained from the methane TPR experiments are presented. Table 4.1 lists temperatures at which variances in pressure occured during each methane TPR and the results of analyses of the final products are shown in Table 4.2.

4.3.1.1 Ni, Mo, Rh

Figure 4.1 shows the methane TPR plot for 9.6% Ni/SiO_2. The 5% Ni/Al_2O_3, 0.5% Rh/Al_2O_3, and 10 to 12% Mo/Al_2O_3 catalysts gave similar curves. For the Ni catalysts, adsorption was evidenced by the decrease in reactor pressure upon contact of CH_4 with the catalyst surface. Gas evolution was first detected at temperatures of 175°C for Ni/Al_2O_3 and 190°C for Ni/SiO_2. Kuijpers and coworkers[11] studied a Ni/SiO_2 catalyst prepared in a similar manner as in this study and found H_2 evolution only at temperatures above 175°C when CH_4 was in contact with the catalyst in a continuous flow system. This is in good agreement with the results observed for the Ni catalysts used in this study. Slightly more CH_4 was observed in the final products for Ni/Al_2O_3 than for Ni/SiO_2. The quantity of H_2, that was estimated in the final products, gave an indication of the degree of methane conversion to *C and H_2. On the Ni catalysts, the methane reaction came very close to reaching thermodynamic equilibrium at 500°C, whereas the methane conversion on Rh and Mo catalysts was far from this. Figure 4.1 also includes a calculated pressure curve over the temperature range representing thermodynamic equilibrium. The reaction on Ni/SiO_2 did not reach equilibrium at any of the temperatures

but came closer at the higher temperatures.

For Mo/Al_2O_3, a decrease in reactor pressure following initial contact of CH_4 with the catalyst signified that adsorption was occuring with little gas evolution. The temperature at the pressure minimum was at approximately 350°C, and rapid increase in pressure followed thereafter for both the Ni and Mo catalysts. The analysis of final products indicated that approximately 70% of the initial CH_4 was present for the Mo catalyst.

Table 4.1 Characteristic Temperatures from the Methane Temperature Programmed Reaction (TPR) profiles.

CATALYST	TEMPERATURE AT INITIAL PRESSURE DECREASE (°C)	TEMPERATURE AT INITIAL PRESSURE INCREASE (°C)	TEMPERATURE AT RAPID PRESSURE INCREASE* (°C)
Ni/Al_2O_3	upon contact	175	---
Ni/SiO_2	upon contact	190	---
Rh/Al_2O_3	upon contact	200	300
Mo/Al_2O_3	upon contact	350	---
Ru/Al_2O_3	--------	190	340
Ir/Al_2O_3	--------	200	420
Re/Al_2O_3	--------	390	---
Pt/Al_2O_3	--------	upon contact	350
Pd/Al_2O_3	--------	upon contact	370
Co/Al_2O_3	--------	upon contact	300
Fe/Al_2O_3	--------	upon contact	380

* if applicable

Table 4.2 Analysis of the Final Products of the Methane TPR.

CATALYST	CH_4[a] (%)	H_2[b]
Ni/Al_2O_3	24	almost all
Ni/SiO_2	16	almost all
Mo/Al_2O_3	70	3/4
Rh/Al_2O_3	50	1/2
Ru/Al_2O_3	48	1/2
Ir/Al_2O_3	45	1/2
Re/Al_2O_3	53	almost all
Co/Al_2O_3	trace[c]	3/4
Pt/Al_2O_3	trace[c]	1/2
Pd/Al_2O_3	49	1/2
Fe/Al_2O_3	47	almost all

[a] relative to the initial pressure of CH_4

[b] amount of H_2 found in the final products in relation to the quantity of H_2 that would have been liberated if all the consumed CH_4 was decomposed to *C and H_2

[c] < 2% initial pressure of CH_4

A slight pressure decrease was found for the Rh catalyst. The minimum pressure occured at 200°C, after which the pressure slowly increased to 300°C. From 300°C to 500°C, the pressure rose rapidly. Approximately 50% of the initial quantity of CH_4 was present in the final products.

The TPR of methane on oxidized Ni/Al_2O_3 and Ni/SiO_2 gave different results from those on the reduced forms. Adsorption of CH_4 slowly increased with temperature but

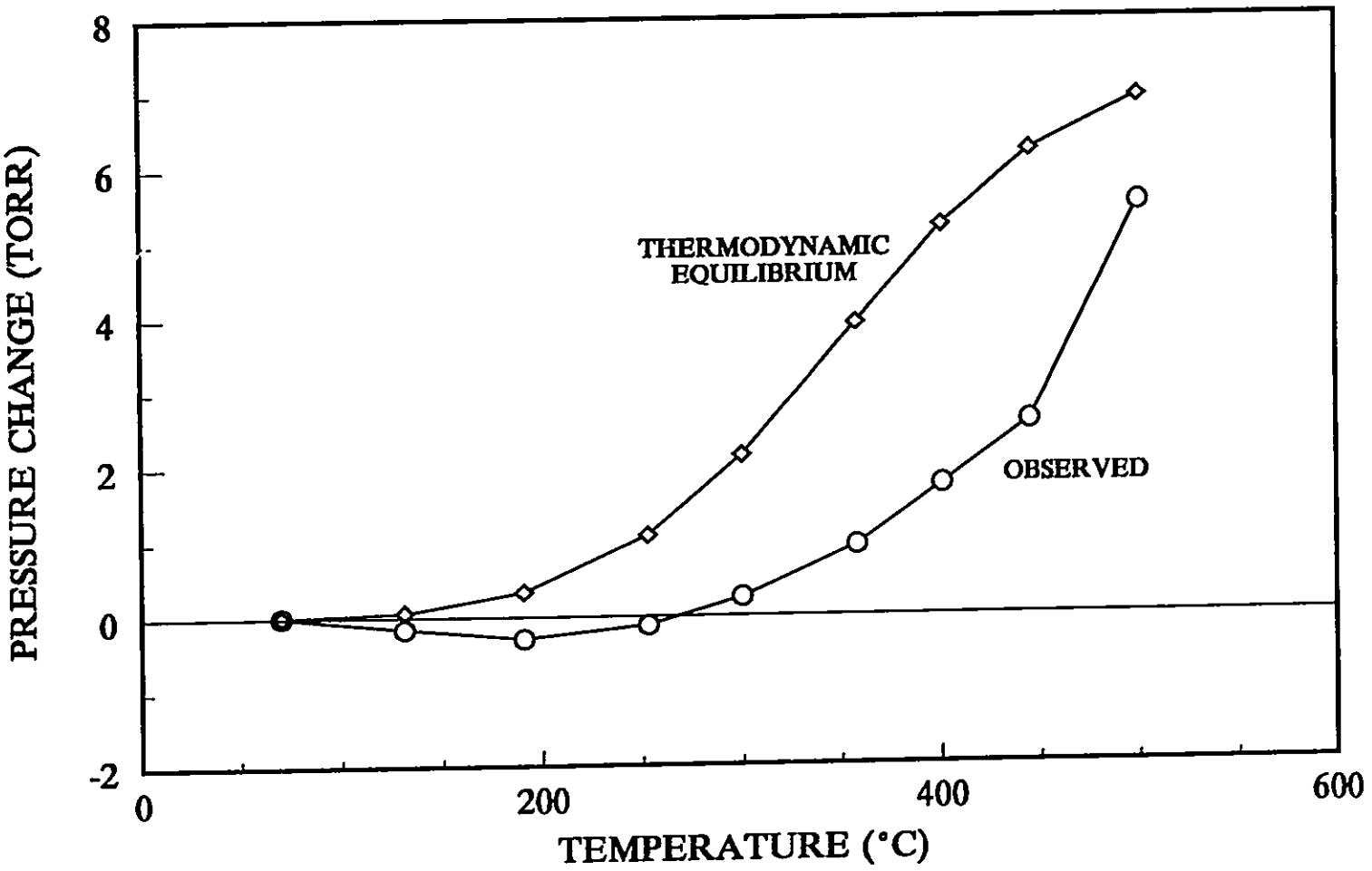

Figure 4.1 Methane TPR profile for 9.6% Ni/SiO_2 and curve representing thermodynamic equilibrium.

not to a very large extent. The oxidized catalysts showed lower amounts of adsorption compared to the reduced catalysts. No decomposition of CH_4 was evident on the NiO/SiO_2 catalyst even at temperatures of 500°C. No CO_2 was detected in the final products, signifying that no reduction of NiO by methane was occuring. For the NiO/Al_2O_3 catalyst, decomposition of adsorbed CH_4 was very pronounced at 440°C with a marked increase in reactor pressure. A large amount of the methane was present in the final products along with some H_2 and a small quantity of CO_2. The large increase in reactor pressure at 440°C is believed to be due to initial reduction of NiO by methane followed by decomposition of some CH_4 on the reduced sites. It appears that dissociation of CH_4 was beginning at these temperatures, releasing hydrogen in the gas phase.

Kuijpers and coworkers[11] have suggested that the low CH_4 conversion at lower temperatures on the Ni catalyst was due to the slow transport of hydrogen (produced during CH_4 dissociation) through the catalyst bed in a coninuous flow system. When the hydrogen stays adsorbed on the catalyst surface, a build up of adsorbed hydrogen causes a shift in equilibrium to the left:

$$CH_4(g) \rightleftharpoons *CH_{(4-x)} + x\ *H \qquad \text{where } 0 < x < 5$$

At higher temperatures, where H_2 begins to desorb, the equilibrium is then shifted to the right.

The reverse process of methane conversion has been observed[17] and formation of CH_4 from $CH_{(4-x)}$ and H_x has been the only product detected from these adsorbed reactants on the Ni catalyst. Higher hydrocarbons have never been found to be products from the

surface reaction of dissociated carbon with hydrogen.

4.3.1.2 Ru, Ir, Re

Figure 4.2 shows the methane TPR curve obtained for 0.5% Ru/Al_2O_3. Similar curves were obtained for Ir/Al_2O_3 and Re/Al_2O_3. Within experimental error, no pressure decrease was observed at low temperatures for these catalysts. The Ru and Ir catalysts began showing methane dissociation with desorption of gas at 190 and 200°C respectively, where reactor pressure started to increase. The increase was gradual at first and then became rapid at higher temperatures (Figure 4.2 for Ru). For the Re catalyst, methane dissociation with gas evolution was not detected until 390°C. This was the highest temperature at which the pressure started increasing compared to the other catalysts studied. Rapid increase in the quantity of desorbed gases occured immediately from 390°C.

Since considerably lower quantities of H_2 were present in the final analysis of gaseous products for Ru/Al_2O_3 and Ir/Al_2O_3 than would be expected if all the consumed CH_4 had decomposed with desorption of H_2, it is believed that some CH_x species (where x=1, 2 or 3) may be present on the catalyst surface.

A large quantity of the initial CH_4 was present in the analysis of final products for all three catalysts. The conversion of methane was 50%, being far from thermodynamic equilibrium (93%) at 500°C.

4.3.1.3 Pt, Pd, Co, Fe

The 1% Pt/Al_2O_3, 0.5% Pd/Al_2O_3, 9.5% Co/Al_2O_3, and 10% Fe/Al_2O_3 catalysts showed similar methane TPR curves. Figure 4.3 is the TPR curve for 9.5% Co/Al_2O_3.

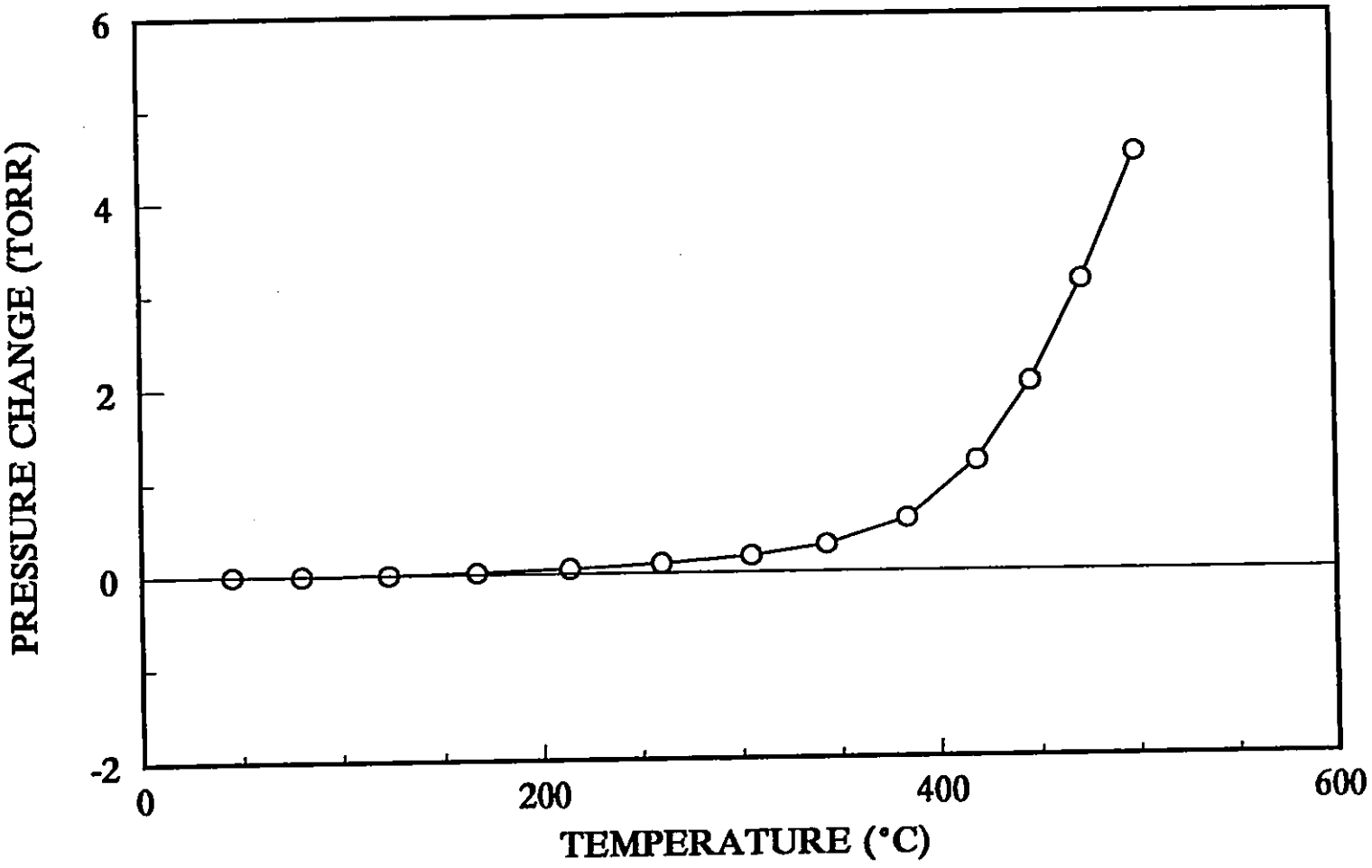

Figure 4.2 Methane TPR profile for 0.5% Ru/Al_2O_3

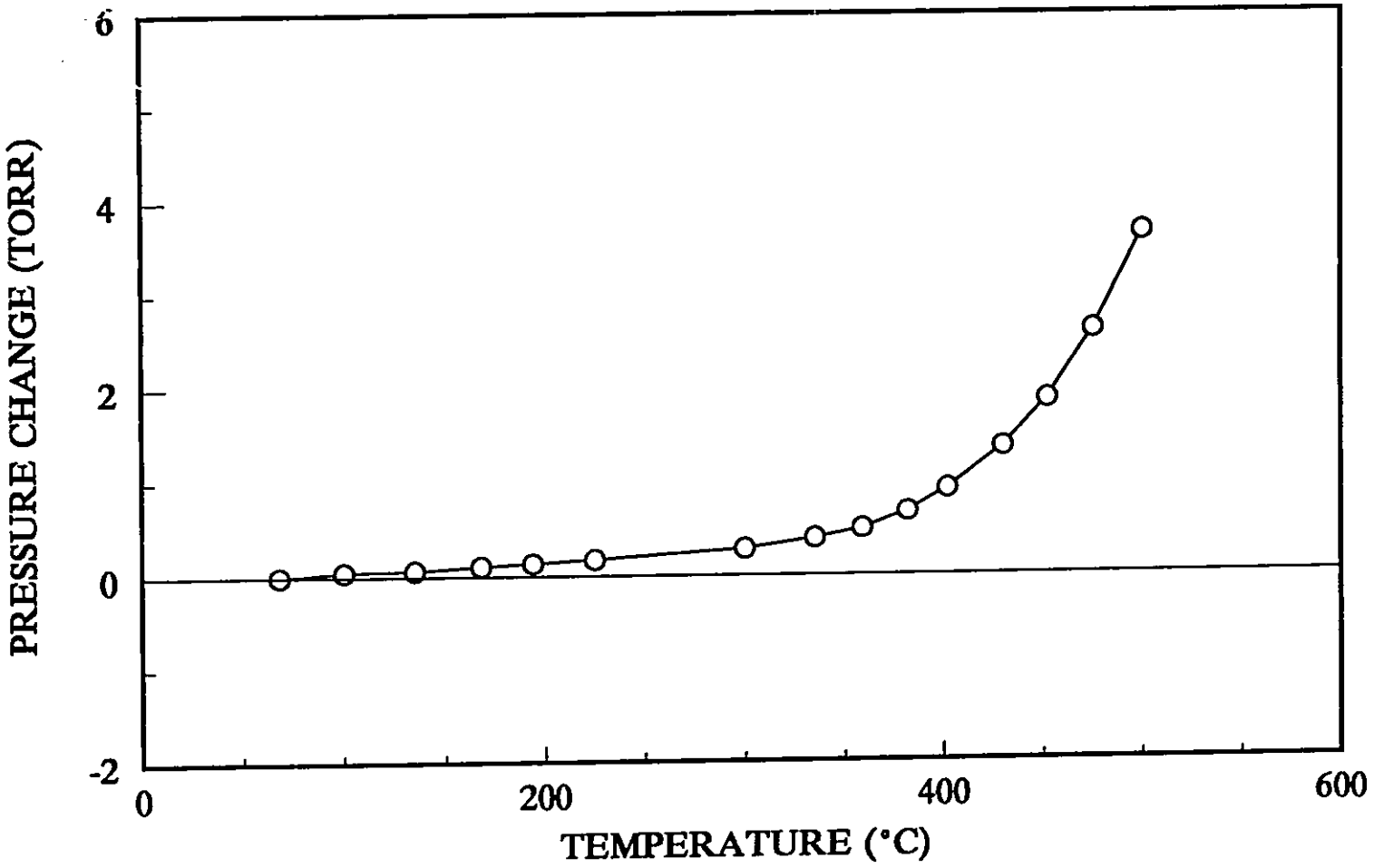

Figure 4.3 Methane TPR profile for 9.5% Co/Al_2O_3

Methane dissociation appeared to occur from initial contact of CH_4 with the catalyst. A rapid increase in reactor pressure occured at various temperatures for the catalysts in this group as is seen in Table 4.1.

For Pt, because of the relatively lower quantity of H_2 found in the final products compared to the near total methane consumption, a considerable quantity of partially dissociated methane species were presumably adsorbed on the catalyst. This was also the case for the Pd catalyst. In the methane TPR experiments for Co and Fe catalysts, 75% or greater of methane that was consumed in the surface reactions had been dissociated to carbon and hydrogen. A trace of CO_2 was detected in the final products for Co, indicating that the catalyst was not completely reduced initially. An increase in reactor pressure occured from the initial contact of CH_4 with the Co catalyst surface, as already mentioned. A slow steady increase was observed up to approximately 300°C. Only a trace of CH_4 was detected in the final products.

For the Fe catalyst, the reactor pressure slowly increased from initial contact of CH_4 with the catalyst to approximately 380°C where a rapid pressure increase began. Approximately 47% of the initial CH_4 was present in the final products. Almost all of the H_2 (compared to the H_2 that would be expected for decomposition of consumed CH_4) was observed suggesting that CH_4 was completely dissociated in the surface reactions.

All of the TPR curves observed in the present study were below the equilibrium curve which is shown in Fig. 4.1. Therefore, decomposition of methane did not reach equilibrium, suggesting that the heating rate during TPR was faster than the rate for the decomposition to reach equilibrium (kinetic control). In order to confirm this, an isothermal reaction was carried out on the Pt/Al_2O_3 catalyst for 60 minutes, at 350°C, using the same quantity of methane as used for TPR. A similar pressure increase to that

observed in TPR at 350°C was reached in 30 minutes. However, the pressure remained unchanged after 30 minutes. At this particular temperature, therefore, the reaction was not controlled by kinetics. Instead, it appears that the surface species formed by the dissociation of methane blocked the surface sites for further reaction. Approximately 50% of the initial CH_4 was detected in the analysis of the final products of the isothermal reaction. A small quantity of H_2 was also detected which may indicate that the majority of the hydrogen produced from the CH_4 dissociation remained adsorbed on the catalyst surface at this temperature as H or CH_n species.

4.3.2 Ethylene TPR Analysis

Thermodynamic calculations show that ethylene decomposition is favoured at the temperatures used in the present work. Examples of typical ethylene TPR curves obtained for the various catalysts are shown. Table 4.3 lists temperatures at which changes in the curves were observed for each catalyst. Table 4.4 shows the results obtained from the G.C. analysis of the final products.

4.3.2.1 Ni, Rh

In Figure 4.4, the ethylene TPR curve for 5% Ni/Al_2O_3 is presented. Similar curves were obtained for 9.6% Ni/SiO_2 and 0.5% Rh/Al_2O_3. Adsorption occured upon initial contact of ethylene with the catalysts. The observed decrease in reactor pressure was the largest for this group compared to that found with the other catalysts that were studied.

5% Ni/Al_2O_3 showed a greater decrease in reactor pressure from initial contact of ethylene with the catalyst even though the Ni/SiO_2 catalyst had more Ni surface sites. Desorption was first observed in the ethylene TPR plots at 150°C for Ni/SiO_2 and 200°C

for Ni/Al_2O_3. The observed reactor pressure increase was slow at first and then became steep. About 20% of the initial ethylene was converted to CH_4 in the final product analysis for Ni/Al_2O_3, and 25% was found for Ni/SiO_2. Therefore C_2H_4 was being cracked during the reactions with Ni.

Table 4.3 Characteristic Temperatures from the Ethylene TPR Profiles.

CATALYST	TEMPERATURE AT INITIAL PRESSURE DECREASE (°C)	TEMPERATURE AT INITIAL PRESSURE INCREASE (°C)
Ni/Al_2O_3	upon contact	200
Ni/SiO_2	upon contact	150
Rh/Al_2O_3	upon contact	340
Mo/Al_2O_3	upon contact	330
Pd/Al_2O_3	130	320
Re/Al_2O_3	upon contact	390
Ir/Al_2O_3	110	320
Pt/Al_2O_3	240	400
Ru/Al_2O_3	upon contact	300
Co/Al_2O_3	--------	upon contact
Fe/Al_2O_3	--------	upon contact

Table 4.4 Analysis of the Final Products of the Ethylene TPR.

CATALYST	C_2H_4[a,b] (%)	CH_4[a,b] (%)	C_2H_6[a,b] (%)	H_2[c]
Ni/Al_2O_3	trace	20	trace	3/4
Ni/SiO_2	trace	25	--	3/4
Rh/Al_2O_3	5	trace	20	1/2
Mo/Al_2O_3	45	trace	15	1/2
Pd/Al_2O_3	15	trace	15	1/2
Re/Al_2O_3	--	10	trace	1/2
Ir/Al_2O_3	30	trace	15	1/2
Pt/Al_2O_3	45	trace	15	3/4
Ru/Al_2O_3	70	trace	trace	3/4
Co/Al_2O_3	--	trace	10	3/4
Fe/Al_2O_3	75	trace	trace	almost all

[a] relative to initial pressure of C_2H_4

[b] trace refers to < 2% of initial pressure of C_2H_4

[c] fraction refers to the amount of H_2 found in the final products in relation to the quantity of H_2 that would have been liberated if all the consumed C_2H_4 was decomposed to *C and H_2

For Rh, the reactor pressure steadily decreased to a minimum at 340°C. The pressure quickly increased from this temperature to the end of the reaction. In the final product analysis about 5% of the initial C_2H_4 and 20% C_2H_6 compared to the initial C_2H_4 was present as shown in Table 4.4. A small trace of CH_4 was detected. The amount of H_2 detected was about 1/2 of H_2 expected if all consumed C_2H_4 had decomposed (taking into

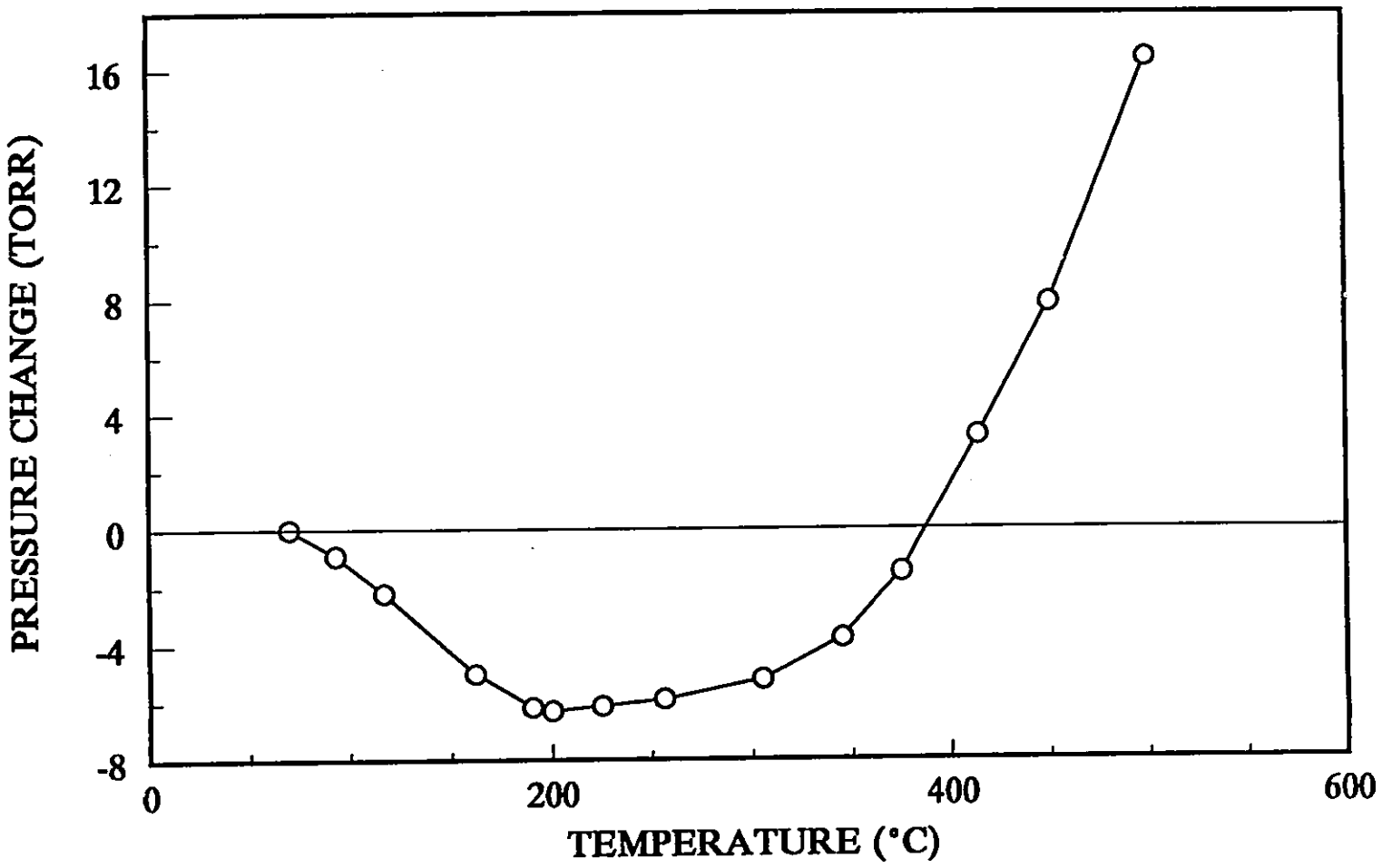

Figure 4.4 Ethylene TPR profile for 5% Ni/Al_2O_3

account the C_2H_4 and H_2 used in the formation of C_2H_6).

For Ni/Al_2O_3, Ni/SiO_2 and Rh/Al_2O_3, the number of surface metal sites on the catalyst contained in the reactor, and the catalyst dispersion, are presented in Table 4.5. As can be seen, Rh/Al_2O_3 showed the smallest decrease in reactor pressure and had the lowest number of metal sites available for adsorption. However, Ni/Al_2O_3 shows the largest decrease in reactor pressure even though the number of surface metal sites available is smaller than for Ni/SiO_2. There appears to be no relationship between the number of surface metal sites and the extent of adsorption of ethylene, as indicated by the maximum decrease in reactor pressure.

Table 4.5 Comparison of Ethylene TPR for 5% Ni/Al_2O_3, 9.6% Ni/SiO_2 and 0.5% Rh/Al_2O_3.

CATALYST	TOTAL NUMBER OF SURFACE METAL SITES[a] (MOLES)	MAXIMUM DECREASE IN REACTOR PRESSURE (TORR)	DISPERSION FACTOR (%)
5% Ni/Al_2O_3	1.610×10^{-5}	6.4	4.1
9.6% Ni/SiO_2	5.822×10^{-5}	4.1	8.2
0.5% Rh/Al_2O_3	4.116×10^{-6}	1.8	17.5

[a] refers to the total number of surface metal sites on the catalyst contained in the reactor

The presence of CH_4 in the final gaseous products could have been the result of decomposition of ethylene directly or via decomposition of ethane. McKee studied adsorption of C_2H_4 and C_2H_6 on unsupported Ni.[47] He argued that CH_4, produced at lower temperatures, is the result of direct C_2H_4 decomposition shown as:

$$C_2H_4(g) \rightleftharpoons CH_4(g) + C$$

This reaction would result in no pressure change. At temperatures above 100°C, McKee observed CH_4 formation from C_2H_6 decomposition. He proposed the following reaction:

$$2\ C_2H_6(g) \rightleftharpoons 3\ CH_4(g) + C$$

which would result in a pressure increase. At 100°C, he found that 2% CH_4 was produced from C_2H_4 and only a trace of CH_4 was observed from C_2H_6 decomposition. Below 100°C, no desorption products were detected from C_2H_6 adsorption on Ni.

From the previous studies using Ni catalysts,[46,47] very little CH_4 is expected to be produced from C_2H_4 decomposition at lower temperatures.[47] The increase in CH_4 production and decomposition to carbon and gaseous H_2 is believed to be responsible for the large increase in reactor pressure observed at higher temperatures.

4.3.2.2 Pd, Mo, Re

The ethylene TPR curve for 0.5% Pd/Al_2O_3 can be seen in Figure 4.5. Similar curves were observed for 10-12% Mo/Al_2O_3 and 0.5% Re/Al_2O_3. The increase in reactor

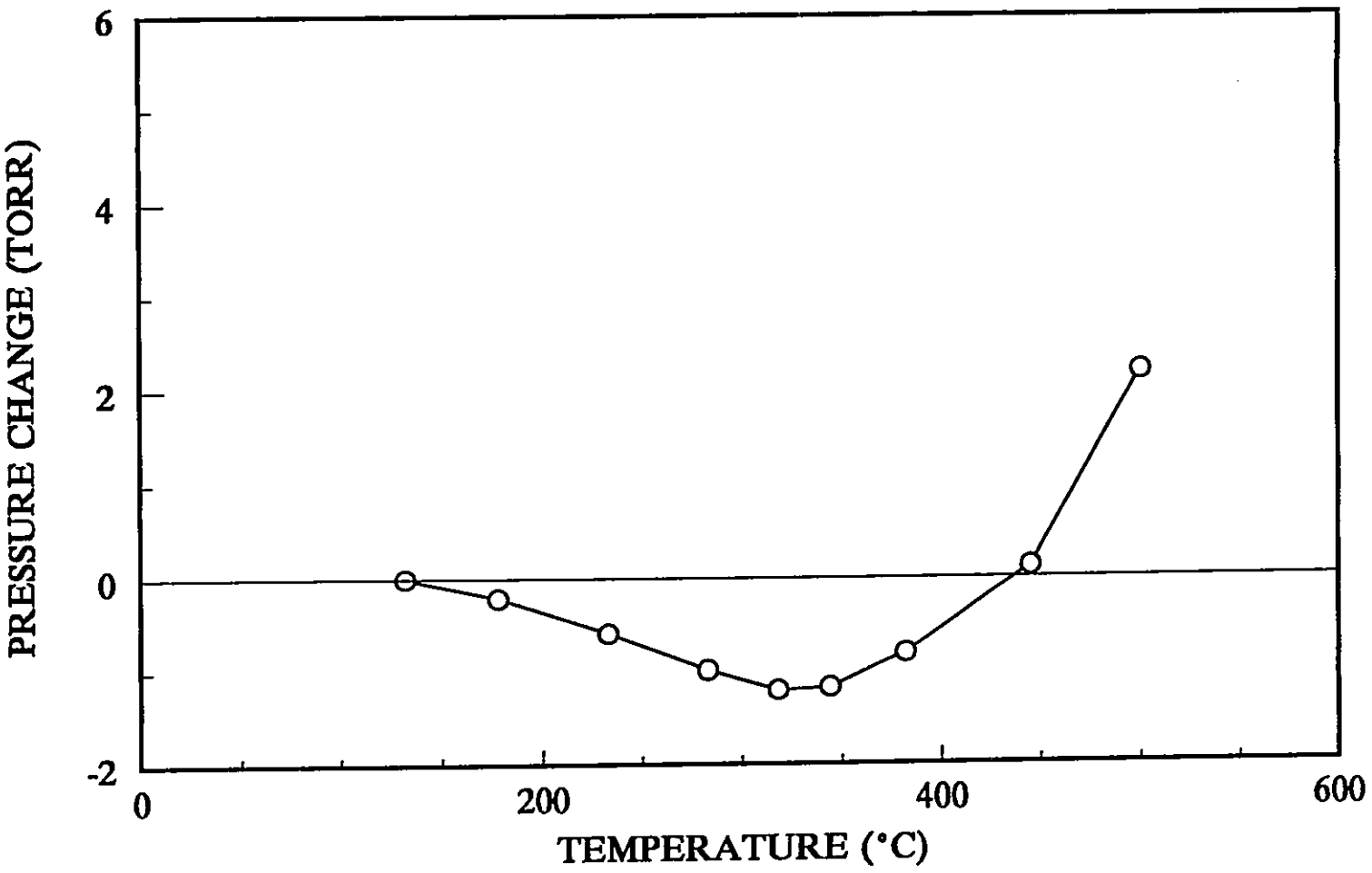

Figure 4.5 Ethylene TPR profile for 0.5% Pd/Al_2O_3

pressure after initial decrease occured at relatively high temperatures compared to other catalysts. The Pd, Re and Mo catalysts showed smaller increases in pressure. For Pd/Al_2O_3, ethylene adsorption was observed at about 130°C. Adsorption increased to a temperature of 320°C. The pressure increased slowly at temperatures above 320°C.

Adsorption of C_2H_4 was observed over a wide range of temperatures for the Mo catalyst. The reactor pressure decreased and reached a minimum at 330°C. The reactor pressure then slowly increased.

For Re/Al_2O_3, adsorption of C_2H_4 occured upon contact of C_2H_4 with the catalyst as observed from the slow decrease in reactor pressure with temperature, reaching a minimum at 390°C. The final analysis of the products revealed that all C_2H_4 was consumed in the TPR and that there was about 10% CH_4, indicating that C_2H_4 cracking was occuring. For all three catalysts, approximately 1/2 of H_2 was present in the final analysis, assuming that all the consumed C_2H_4 had completely dissociated to carbon and gaseous H_2.

4.3.2.3 Ir,Pt

Figure 4.6 shows the ethylene TPR curve for 1% Ir/Al_2O_3. A similarly shaped curve was observed for 1% Pt/Al_2O_3. Appreciable adsorption of ethylene was first detected at 110°C for the Ir catalyst but not until 240°C for Pt/Al_2O_3. Both showed small decreases in reactor pressure compared to other TPR curves, suggesting that there probably was very little ethylene adsorption. As seen in Table 4.3, pressure increase was seen at 320°C for Ir but not until 400°C for Pt. Considerable amounts of C_2H_4 were detected in the final products for both catalysts (30% and 45% for Ir and Pt respectively).

Isothermal reactions of C_2H_4 in contact with the Pt catalyst at 150°C and 350°C were

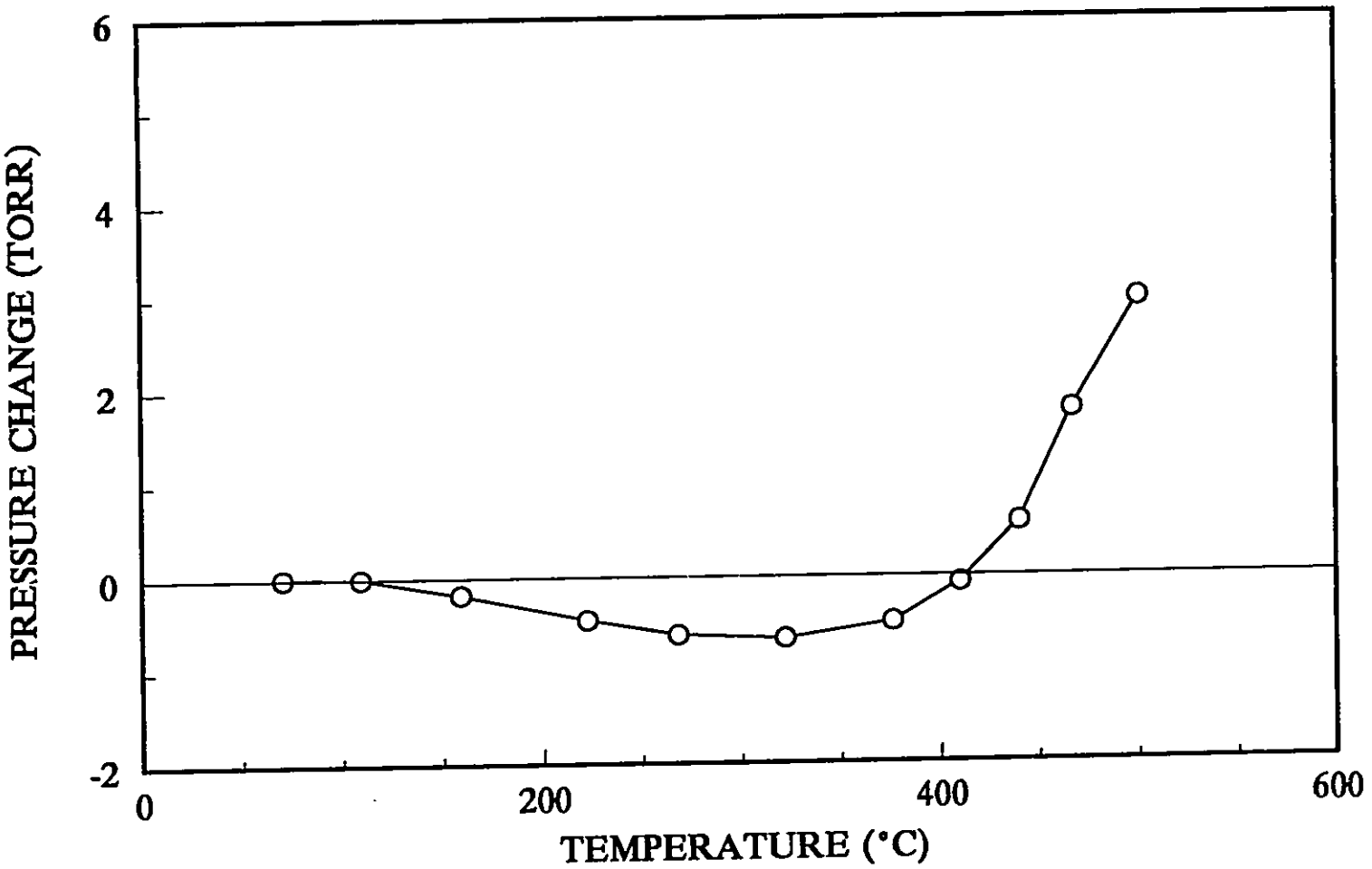

Figure 4.6 Ethylene TPR profile for 1% Ir/Al_2O_3

carried out. Table 4.6 lists the final products that were detected in the isothermal reactions and TPR for Pt/Al_2O_3. At 150°C, there was no change in reactor pressure during the 60 minutes that C_2H_4 was in contact with the catalyst. At the end of the isothermal reaction, 86% of the original C_2H_4 was present and the balance was assumed to be mainly H_2 with a trace of CH_4 and C_2H_6.

Table 4.6 Final Products of Ethylene Reactions on 1% Pt/Al_2O_3.

FINAL PRODUCTS	TPR (%)[a,b]	ISOTHERMAL REACTION AT 150°C (%)[a,b]	ISOTHERMAL REACTION AT 350°C (%)[a,b]
C_2H_4	45	86	77
C_2H_6	15	trace	6
CH_4	trace	trace	trace

[a] the percentage of products is that compared to the initial pressure of C_2H_4 and the remainder is the consumed C_2H_4 that was not detected in the gas phase

[b] trace refers to < 2% of initial C_2H_4 pressure

The reactor pressure steadily decreased over time during the isothermal reaction at 350°C. The adsorption did not appear to reach equilibrium after 60 minutes since the reactor pressure did not stabilize. Also, after 60 minutes the pressure decrease was three times greater than that which was observed from the ethylene TPR at 350°C. At the end

of the isothermal reaction, 77% of the initial C_2H_4 was present, along with 6% C_2H_6. A trace of CH_4 was also detected. An additional reaction was carried out at 350°C, but in this case the catalyst was previously reduced with CH_4 at 475°C instead of H_2 at 400°C. An identical curve was obtained as that of the previous isothermal reaction at 350°C as well as similar quantities of final products.

An additional ethylene TPR was carried out after pretreating the Pt catalyst in air at 550°C, followed by evacuation at the same temperature. Ethylene adsorption began upon contact of C_2H_4 with the catalyst and increased to a temperature of 390°C. Above 390°C, the pressure quickly increased. Mostly CH_4 was detected in the final products along with some C_2H_6. Therefore C_2H_4 was being decomposed on the surface and some ethylene self-hydrogenation was occuring. A considerable amount of dissociated ethylene must have been left on the catalyst surface because no C_2H_4 was detected in the gas phase and the CH_4 and C_2H_6 in the final products accounted for a small part of the consumed C_2H_4. The hydrogen adsorption isotherm of Pt/Al_2O_3 pretreated in air showed that the number of active metal sites had not been altered from that observed with the same catalyst previously reduced in H_2. Therefore air pretreatment does not appear to change the surface metal sites. Rickard *et al.*[53] found that at temperatures below 450°C, O_2 contact with supported Pt did not show any significant modification in crystallite size. Also, below 550°C, they did not observe electron diffraction patterns for oxides such as PtO, PtO_2, or Pt_3O_4. These observations are in agreement with the present study showing that O_2 contact with Pt crystallites does not affect the metal active sites.

4.3.2.3 Ru

A unique TPR curve was obtained for 0.5% Ru/Al_2O_3. After an initial pressure

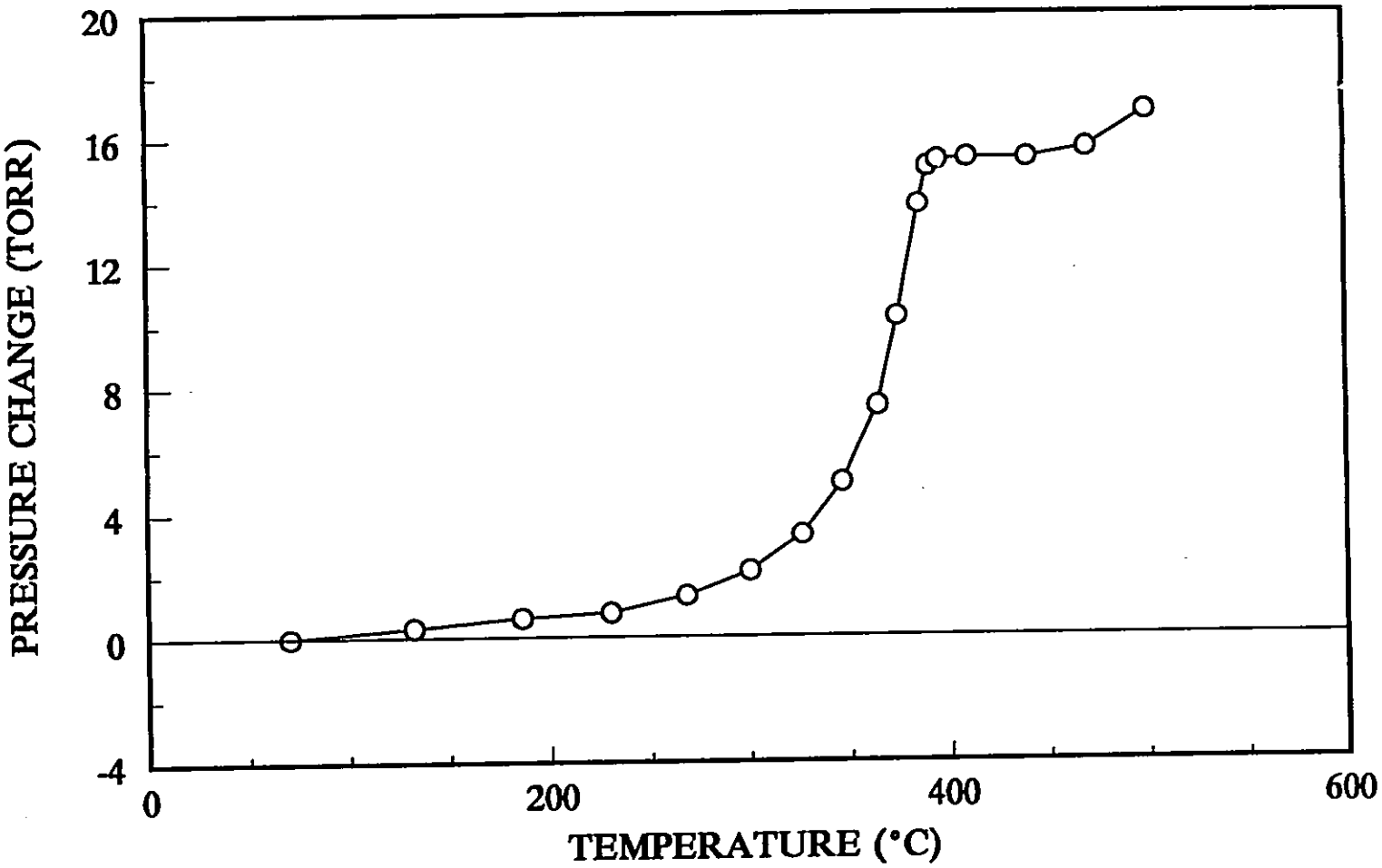

Figure 4.7 Ethylene TPR profile for 9.6% Co/Al_2O_3

decrease, no variation in the reactor pressure was observed up to a temperature of 300°C. Above 300°C, the reactor pressure increased, indicating decomposition of C_2H_4. Even after reaching temperatures of 500°C, about 70% of the initial C_2H_4 was present in the final products. A trace of C_2H_6 was observed as well as a trace of CH_4. The quantity of H_2 was found to be about 3/4 of H_2 if all the consumed ethylene was dissociated to carbon and hydrogen. Ethylene self-hydrogenation was occuring to some extent.

4.3.2.4 Co, Fe

The ethylene TPR curve for 9.6% Co/Al_2O_3 is shown in Figure 4.7. The slow increase in reactor pressure, upon contact of ethylene with the catalyst, was also seen for 10% Fe/Al_2O_3. A sharp increase in reactor pressure was observed for Fe, but the increase did not level off towards the end of the TPR as was seen with the Co catalyst (refer to Table 4.3). The levelling off of the reactor pressure and the fact that no ethylene was detected in the final products suggest that surface reactions reached completion before the end of the TPR. A trace of CH_4 was detected in the final products, indicating that ethylene was being cracked. For the Fe catalyst, a very large quantity of ethylene remained after the TPR as seen in Table 4.4. These facts indicate that ethylene decomposition is slower on Fe compared to Co, and is not completed at the end of the TPR. This was similar for Ru where decomposition was even slower than with the Fe catalyst at low temperatures. Evidence of ethylene self-hydrogenation was found for both catalysts.

4.4 SUMMARY

Temperatures at which adsorption and decomposition of reactants were first detected

were of special interest. There is a possibility, from analysis of the final products of the TPR experiments, that methane forms partially dissociated species on some of the catalysts. Methane and ethylene reactivities varied on the different catalysts studied. Very little activity was observed on some catalysts such as Fe/Al_2O_3, while others showed conversions approaching thermodynamic equilibrium, as for instance methane in contact with Ni/Al_2O_3.

Chapter 5

ISOTHERMAL REACTIONS OF METHANE ON SUPPORTED METAL CATALYSTS

5.1 INTRODUCTION

The catalytic formation of ethane from methane has not been previously observed using metal catalysts on oxide supports at conventional reaction conditions, although thermodynamically it is possible. Keller and Bhasin found ethylene formation from the oxidative coupling of methane which involved the oxygen of the metal oxide catalysts.[2] Very low conversions were observed at temperatures above 800°C and pressures of one atmosphere. Oxides of Sn, Pb, Sb, Bi, Tl, Cd, and Mn supported on alumina were found to be active. Also, Olah has converted natural gas to higher hydrocarbons using solid superacids.[54] He found that conversion of methane can occur in the absence of olefins when initiated by a hydrogen acceptor (O, Cl, S, or Se) or HX (X = Cl or F).

In the present study, in trying to increase the yield of ethane to detectable levels, the ethane that was produced was continuously removed from the gas phase while the methane pressure was kept constant. This was accomplished by placing a liquid N_2 trap in the circulation system. The vapour pressure of methane above liquid N_2 is 9.6 torr, therefore, about 20 torr of methane was placed in the reactor system to ensure that ample quantities of reactant were available. As described in Chapter 1, two reactions, the decomposition of methane and the formation of ethane, take place competitively. The replenishment of methane would drive the simultaneous reactions (K_1, K_2) to the right. Also, ethane was removed from the gas phase, which would cause the reaction in K_2 to

be driven to the right. It must be noted though, that the vapour pressure of ethane above liquid N_2 is of the order of $1x10^{-3}$ torr which corresponds to $3x10^{-9}$ moles in the present reaction system. If less than this quantity of ethane is present during the reaction, then none of the ethane would be removed from the gas phase, and an attempt to remove ethane to drive the K_2 reaction to the right would be unsuccessful.

For some of the catalysts studied, the amount of carbon (C, CH, CH_2, CH_3) interacting with the surface during these reactions was determined by oxidizing the catalysts after stopping the reaction and analyzing the CO_2 that was produced.

5.2 EXPERIMENTAL PROCEDURE

5.2.1 Isothermal Methane Reaction at 250°C and 500°C

Each catalyst was reduced for 1 hour at 500°C, then evacuated for 30 minutes while being cooled to the reaction temperature. Methane (3% of total gas pressure) mixed with helium was added to the circulation system ($V_1+V_2+V_C$). Helium was added to the system to increase the efficiency of the circulation. A liquid N_2 trap was used to keep methane at its vapour pressure of 9.6 torr. While circulating, the gas mixture was expanded to the reactor. The reaction was continued for 90 minutes (or in one case 60 minutes). A G.C. analysis was obtained of the condensable gaseous products.

5.2.2 Oxidation of Catalysts

Some catalysts were oxidized at 500°C after stopping the isothermal methane reaction. Pure oxygen, at 150 torr, was circulated over the catalyst at 500°C for 30 minutes. A liquid N_2 trap was used to condense the CO_2 that was produced. After 30 minutes, the

reactor system was evacuated. The condensed CO_2 was then vapourized and analyzed.

5.3 RESULTS

The methane reaction at 250°C showed no evidence of ethane formation with any of the catalysts. This indicates that less than $1x10^{-3}$ torr ($3x10^{-9}$ moles), if any, of ethane was being produced in the system. For all catalysts studied, except Fe/Al_2O_3, varying quantities of ethane were detected from methane reactions at 500°C. Table 5.1 presents the results of methane reactions at 500°C and consequent surface carbon analyses. The turnover frequency (TOF) of methane producing ethane was calculated as well as the TOF of methane producing surface carbon (C, CH, CH_2, CH_3). It was assumed that the reactions proceeded steadily over the reaction time employed. From the quantities of ethane produced, it is evident that the reaction of K_2 was shifted to the right by driving the reaction from equilibrium via methane replenishment and ethane removal. Under the conditions of the experiment, carbide formation could not be directly determined since oxidation of the catalyst surface removed not only carbide but also CH_n species as CO_2.

It is possible that the speed of the circulation pump may affect the amount of ethane formed if equilibrium is established in the reaction. This is only a concern for the catalysts showing the largest amount of ethane and surface carbon formed. Reaction rates of any of the other catalysts producing lower amounts of ethane are ensured not to be limited by the flow rate since higher rates of reaction have been observed using the same pumping speed.

The TOF for ethane formation at 500°C decreased in the following order:

$$Ru > Re > Rh > Pd > Ir > Pt > Co > Ni$$

No indication of ethane formation was observed for the Fe catalyst. The decreasing order for surface carbon formation at 500°C was found to be:

$$Fe > Pd > Ni > Ir > Pt > Re$$

Table 5.1 Results of Isothermal Methane Reactions at 500°C[a].

CATALYST[b]	MASS OF CATALYST IN REACTOR (g)	ETHANE PRODUCED (moles/g)	SURFACE CARBON PRODUCED (moles/g)	TOF[c] FOR ETHANE PRODUCTION	TOF[c] FOR SURFACE CARBON[d] PRODUCTION
Ni 5.0%	0.2043	5.372×10^{-6}	1.489×10^{-4}	6.869×10^{-5}	9.518×10^{-4}
Rh 0.5%	0.4836	9.543×10^{-6}		6.229×10^{-4}	
Ir 1.0%	0.4563	1.011×10^{-5}	2.717×10^{-5}	1.987×10^{-4}	5.581×10^{-4}
Ru 0.5%	0.4361	1.852×10^{-5}		4.544×10^{-3}	
Re 0.5%	0.4023	2.051×10^{-5}	1.291×10^{-5}	9.040×10^{-4}[e]	2.905×10^{-4}[e]
Pt 1.0%	0.3768	3.041×10^{-5}	1.080×10^{-4}	1.103×10^{-4}	3.915×10^{-4}
Pd 0.5%	0.5225	1.435×10^{-5}	1.833×10^{-4}	3.671×10^{-4}	2.343×10^{-3}
Co 9.5%	1.0910	7.366×10^{-6}		8.042×10^{-5}	
Fe 10.0%	0.3965	------	4.494×10^{-4}	------	3.989×10^{-3}

[a] reaction times were 90 min except in the case of Rh for which reaction time was 60 min

[b] all catalysts were supported on Al_2O_3 on a w/w basis

[c] molecules/(s site)

[d] surface carbon may be in the form of *C, *CH, *CH_2, or *CH_3

[e] the dispersion of Re was assumed to be the same as that of Pd

5.4 DISCUSSION

As already mentioned, the formation of ethane from methane was driven away from equilibrium in the direction of K_2 in the hopes that detectable quantities of ethane could be observed. The attempt was successful for reactions occuring at 500°C. Ethane was not detected in the final products for the reactions carried out at 250°C. As seen in Table 1.1, K_2 increases with temperature, although in this temperature range, K_2 remains very small especially in comparison to K_1. K_1 increases in magnitude at a much greater rate with temperature than does K_2. Therefore, the calculated conversion to ethane in the multi-equilibria system is larger at 250°C than at 500°C. It would be expected, then, that more ethane would be produced at 250°C than 500°C in the driven reaction. Since this was not the case, and the reaction was not limited by the speed of circulation, ethane production must be controlled by kinetics. The formation of ethane could occur in two possible mechanisms. A methane molecule in the gas phase could interact with an adsorbed methane species (Rideal-Eley Mechanism), for instance:

$$CH_4(g) + *CH_n \rightleftharpoons C_2H_6(g) + (n-2)\ *H \qquad n=1,2,3$$

In this case the reaction process would be, in part, dependent upon the quantity of partially dissociated species present on the catalyst surface.

A second possible mechanism would involve interaction of two adsorbed methane species (Langmuir-Hinshelwood Mechanism). An example would be:

$$2\ *CH_3 \rightleftharpoons C_2H_6\ (g)$$

For the Langmuir-Hinshelwood mechanism, the two methyl species must be in close proximity for interaction to occur. An isothermal adsorption of methane, carried out at room temperature, showed one molecule adsorbed per 120 surface metal sites. At higher temperatures, still fewer adsorbed species would be expected. Therefore, the adsorbed methane species must be very mobile in order for the reaction to proceed readily. Since ethane was observed only at 500°C, this may suggest that the mobility of the methane surface species had increased suitably enough (as compared to the reaction at 250°C) to form detectable amounts of ethane.

By viewing the conversion of methane for both cases under equilibrium conditions seen in Table 1.1, it is evident that under the non-equilibrium conditions, ethane production was greatly increased. The TOF of surface carbon formation was still much larger than the TOF for ethane production with regard to each catalyst. (It must be kept in mind that under the experimental conditions, the TOF of surface carbon formation includes not only carbide formation but also any partially dissociated methane species on the surface).

The results have shown that when the TOF of a given catalyst for producing ethane is high, the TOF for producing surface carbon is relatively low. The largest quantity of surface carbon was formed on iron. The methane TPR analysis of Fe/Al_2O_3 showed that after reaching a reaction temperature of 500°C, almost all of the methane consumed (53%) had completely dissociated to carbon and gaseous H_2 (Table 4.2). The Ni/Al_2O_3 catalyst showed the third highest TOF for surface carbon formation. In the TPR analysis of both Ni catalysts, methane conversion to carbon and gaseous H_2 came closer to reaching thermodynamic equilibrium than any of the other catalysts. This result is supported by the methane isothermal reaction results on Ni at 500°C where there was a large production

of surface carbon. It may have been expected, when comparing the TPR results, that the Ni catalyst should have produced more surface carbon over the same period of time as compared to Fe/Al_2O_3. Over the 90 minute reaction time at 500°C, the Fe catalyst produced surface carbon at a faster rate than Ni/Al_2O_3. With the TPR experiments, the reaction was stopped once the temperature reached 500°C. Both the Ni and Fe catalysts showed large increases in pressure up to this temperature with Fe showing initial increase at a much higher temperature. The temperature range of accelerated dissociation of methane was much larger for Ni than Fe up to 500°C. The explanation for the discrepancy is that during the TPR reactions up to 500°C, Ni catalysts produced more surface carbon, but at the prolonged isothermal temperature of 500°C, Fe/Al_2O_3 showed a higher rate of reaction. This would mean that at a temperature between the initial accelerated increase (380°C) in the complete dissociation of methane and the final temperature (500°C), the rate of surface carbon formation for Fe/Al_2O_3 overtakes that of Ni/Al_2O_3. From the TPR, the integrated amount of carbon produced over a range of temperatures is determined. The isothermal study determined the amount of carbon produced at 500°C for 90 minutes.

Complete dissociation of methane to carbon and H_2 was found to be the predominant reaction on the Ni and Fe catalyst surfaces from the TPR analyses. Therefore it is not surprising that ethane was not observed as a final product of the reaction at 500°C on Fe/Al_2O_3 and that Ni/Al_2O_3 showed the lowest TOF of ethane formation of any of the other catalysts. The presence of partially dissociated methane species ($*CH_n$) is essential for ethane production.

Pd/Al_2O_3 showed a slightly higher TOF for surface carbon formation than Ni/Al_2O_3, followed by Ir/Al_2O_3. The Pd and Ir catalysts showed an approximate 45 to 50%

conversion of initial methane in the TPR anaylsis (Table 4.2). Re/Al_2O_3 showed the lowest TOF for surface carbon formation of the catalysts analysed, and also showed a relatively high TOF for ethane production (Table 5.1).

5.5 SUMMARY

Ethane was observed as a product of methane interaction with the supported catalyst surface at 500°C when driven away from thermodynamic equilibrium, with TOF in the following order:

$$Ru > Re > Rh > Pd > Ir > Pt > Co > Ni$$

No ethane formation was observed for Fe. In the same experiment, the order of TOF for surface carbon formation was found to be:

$$Fe > Pd > Ni > Ir > Pt > Re$$

From thermodynamic calculations of the simultaneous equilibrium of ethane formation and complete methane dissociation (as shown in Table 1.1), one would expect to see more ethane produced at lower temperatures. Experimentally, ethane was only observed at 500°C and not at 250°C. This indicates that the process of ethane formation is kinetically controlled.

Chapter 6

METHANE-ETHYLENE COUPLING REACTIONS

6.1 INTRODUCTION

The coupling of methane with ethylene in the presence of a catalyst to form higher hydrocarbons has many competing reactions. These include such processes as decomposition, and oligomerization of ethylene. As discussed in Chapter 1, the methane-ethylene coupling reaction is thermodynamically more favourable than the methane decomposition reaction at temperatures below 400°C. The reaction of ethylene oligomerization and ethylene decomposition to carbon and hydrogen, however, are more favourable than the coupling reaction in this temperature range (see Figure 1.1).

Scurrell and coworkers have observed methane-ethylene coupling over a sulphate treated zirconia catalyst, obtaining C_6 and C_7 products.[6] Siskin[3] and Sommer[4] have used liquid superacids to successfully couple methane and ethylene. Olah and coworkers[5] have accomplished the same using solid superacids. Details of the experiments were described more completely in Chapter 1. In a recent study,[7] the coupling of methane and propylene on Ni/SiO_2 at 350°C was reported with an 81.4% selectivity to butane when the catalyst was activated with CH_4. For Ni/Al_2O_3, using the same reaction conditions, a 51.7% selectivity to butane was obtained. It was determined, however, that the reaction on this catalyst producing butane only involved propylene and not methane-propylene coupling. All work[7,8] using supported nickel catalysts reported that the catalysts were activated only after they were treated with methane at high temperature to deposit carboneous materials on the surface. In addition, both reports lacked the information on

the precise material balance. Certainly, more study is needed to develop this process.

In the present study, mixtures of methane and ethylene were circulated over various transition metal catalysts at temperatures in the range of 200 to 400°C to determine if any methane-ethylene coupling was occuring.

6.2 EXPERIMENTAL PROCEDURE

The catalysts were reduced at 400°C and evacuated before each experimental run unless otherwise stated. The methane and ethylene reactants were well mixed by circulation before being introduced to the reactor system (methane 95%, ethylene 5%). The partial pressures of methane and ethylene were 254 torr and 13 torr, respectively. The weight of the catalyst sample used was about 0.5 g.

The reactant mixture was circulated over the catalyst for 30 minutes at the reaction temperature and the final gas mixture was analysed by gas chromatography.

6.3 RESULTS

The reaction products were studied in order to detect the presence of higher hydrocarbons which may have formed due to methane-ethylene coupling. Reaction temperatures were generally between 200 and 350°C. The methane-ethylene coupling is thermodynamically more favourable at lower temperatures (Table 6.1 and Figure 1.1), although the temperature should be kept as high as possible in order to have a high efficiency of catalytic conversion.

The catalyst supports were first tested to determine if they were active under these reaction conditions. Samples of Al_2O_3, reduced at 400 and 600°C, were run at 150, 250 and 350°C. Al_2O_3 showed complete inactivity at all these temperatures. SiO_2 was

reduced at 500°C and runs were carried out at 250 and 350°C. SiO_2 also showed no activity at these temperatures.

Table 6.1 Thermodynamic Data for the Coupling Reaction: $CH_4 + C_2H_4 \rightleftharpoons C_3H_8$.

TEMP (°C)	ΔG_r (kcal)	K
250	-2.420	1.026×10^{1}
300	-0.790	2.001×10^{0}
350	0.831	5.112×10^{-1}
400	2.441	1.612×10^{-1}
450	4.050	5.967×10^{-2}

The methane concentration remained unchanged, within experimental error, in all cases. Under these conditions, even if all the ethylene was converted to methane, the methane partial pressure would only increase by about 5%. The gas chromatograph was not accurate enough to detect such a small change in an excess of methane. Therefore, quantitative data relating to the possible conversion of methane and also the conversion of ethylene to methane during the coupling reactions could not be obtained.

Table 6.2 summarizes the results obtained from the coupling experiments. These results are discussed in more detail below for each catalyst. In some instances, the TCD detected a much lower quantity of methane in the final products compared to the FID. The TCD gives a negative peak area for hydrogen, and hydrogen and methane were not

Table 6.2 Results of Methane-Ethylene Coupling Reactions[e].

CATALYST	TEMP (°C)	% C_2H_4[a]	% C_2H_6[a]	% C_3H_6[a]	% C_3H_8[a]
Ni/Al_2O_3	250	--	55	--	--
	300	--	36	--	--
	250[b]	--	--	--	--
	350[b]	--	--	--	--
NiO/Al_2O_3	300	87	--	--	--
	350	79	trace	--	--
Ni/SiO_2	250	--	45	--	--
	350	--	trace	--	--
	250[b]	--	--	--	--
	350[b]	--	--	--	--
	250[c]	--	--	--	--
	350[c]	--	--	--	--
Pt/Al_2O_3	250[b]	--	present	--	present
	350[b]	--	present	--	--
	350[b,d]	--	present	--	--
Mo/Al_2O_3	250	82	28	--	--
	300	55	31	--	--
	250[b]	present	--	--	--
	350[b]	present	present	--	--
	300[d]	83	--	--	--
	350[d]	84	--	--	--
Ir/Al_2O_3	250[b]	--	--	--	--
	350[b]	--	--	--	--
Co/Al_2O_3	200	79	trace	trace	--
	250	76	21	trace	--
	350	--	trace	--	--
Fe/Al_2O_3	250	100	--	--	--
	350	93	--	--	--

[a] relative to initial ethylene used
[b] quantity of ethylene sufficient to cover 50% of metal sites: only qualitative analyses were performed for these reactions
[c] quantity of ethylene sufficient to cover 25% of metal sites
[d] catalyst was pretreated in air
[e] trace refers to a quantity < 2% of initial ethylene used

separated with the G.C. column employed. When the FID indicated that much more methane was detected compared to the TCD, then hydrogen was assumed to be interfering with the methane peak of the TCD.

6.3.1 5% Ni/Al_2O_3

For the reactions at 250 and 300°C, ethylene was completely removed from the gas phase and ethane was detected. Approximately 55% of the initial ethylene had been hydrogenated to ethane at 250°C, this being 36% for the reaction at 300°C. At both temperatures, the remainder of the ethylene was presumably adsorbed on the catalyst.

Experimental runs were also carried out where the number of ethylene molecules admitted into the reactor system was chosen to be equal to 50% of the active metal sites available on the catalyst. This would ensure that ethylene did not completely cover all of the active sites, thus leaving some sites free for methane adsorption. It would also enable adsorbed species to have some mobility. This quantity of ethylene was much lower than that used under standard conditions. In these cases, the amount of ethylene used ranged from 0.5 to 2% of the total reactant pressure whereas for the standard reaction, ethylene was 5% of the total reactant pressure.

At reaction temperatures of 250 or 350°C, all ethylene was adsorbed on the catalyst, and ethane was not detected in the final products. Hydrogen peak interferences with the methane peak from the TCD revealed that hydrogen was present. Hydrogen was not detected in reactions run at the same temperatures but using larger quantities of ethylene. It is possible that the H_2, which might have been liberated when excess C_2H_4 was used, was consumed by the hydrogenation of C_2H_4.

The Ni/Al_2O_3 catalyst was also oxidized in air at 500°C. A reaction was carried out

at 300 or 350°C and the G.C. analysis of the final products verified that the concentration of ethylene decreased slightly. No other products were detected and we conclude that the NiO catalyst is inactive.

6.3.2 9.6% Ni/SiO_2

Under the standard reaction conditions at 250 or 350°C, no ethylene remained in the gas phase. A small amount of ethane was detected from the final products of the reaction at 350°C, but about 45% of the initial ethylene was converted to ethane in the reaction at 250°C.

Reactions were also carried out where the quantity of ethylene used was equal to 50% and 25% of the active metal sites contained in the reactor. These reactions were run at 250°C or 350°C. Only hydrogen and methane were detected in the gas phase.

6.3.3 1% Pt/Al_2O_3

The reactions were carried out at various temperatures between 150 and 350°C using low concentrations of ethylene. For reactions at 150 and 200°C, very little of the ethylene was consumed. Only at temperatures above 200°C was all of the initial ethylene consumed during the reaction. Small quantities of ethane were produced in both reactions, indicating the occurence of ethylene hydrogenation. Because of the differences in quantity of methane detected by the FID and TCD, hydrogen was noted to be present.

For reactions carried out below 250°C, ethane was observed in increasing quantities with increase in reaction temperature. The reaction at 250°C showed the presence of propane in the final products. For reactions carried out at temperatures above 250°C, all ethylene was consumed. Propane was only observed with the Pt catalyst and only at

250°C. Repeated runs at 250°C gave identical results. Therefore, we believe that propane was produced from methane-ethylene coupling. The production of propane is thermodynamically more favourable at 250°C than at 350°C which may account for these results. Kinetic limitations may be responsible for the absence of propane in the final products for reactions carried out at lower temperatures than 250°C.

A reaction at 350°C was carried out after the catalyst had been in contact with air at 500°C. The resulting final products were similar to that found for the reduced catalyst, indicating that oxygen appears to have no effect on the catalyst activity.

6.3.4 10 to 12% Mo/Al_2O_3

The Mo catalyst appeared to have low activity for ethylene adsorption because ethylene still remained as a final product, not only for the reactions carried out under the standard reactant ratios, but also when only small quantities of ethylene were used. For the reactions with small quantities of ethylene reactant, which were carried out at 250 and 350°C, hydrogen was detected in the gas phase. Ethane was observed in the reaction at 350°C when very little ethylene reactant was used (50% of sites covered), indicating that some ethylene was being hydrogenated.

Ethylene hydrogenation was occuring in the reactions at 250 and 300°C under general reaction conditions. Approximately 30% of the initial ethylene in the 250 and 300°C reactions was converted to ethane. Hydrogen was not detected in the final products.

Reactions were run at 300 and 350°C after the catalyst had been treated in air at 500°C. No reaction was observed. Final product analysis showed that small amounts of ethylene were adsorbed on the catalyst.

6.3.5 1% Ir/Al_2O_3

The reactions were carried out at 250 and 350°C. Similar results were obtained in both cases. The ethylene was completely removed from the gas phase by the end of the reaction. H_2 was present in the gas phase but no ethane was detected.

6.3.6 9.5% Co/Al_2O_3

A trace of propylene was detected in reactions carried out at 200 and 250°C. Only a small quantity of ethylene was consumed during the reactions. Very little hydrogenation occured. The reaction at 350°C gave very different results. Ethylene was completely consumed during the reaction and propylene could not be detected in the final products. Hydrogen was detected in the final products of all reactions.

The propylene could possibly be formed from the oligomerization of ethylene followed by cracking to form propylene. Propylene was only observed at temperatures at or below 250°C. Thermodynamic equilibrium for ethylene oligomerization increases with decreasing temperature, so under experimental conditions, propylene was not being produced at temperatures above 250°C. Another possibility for the absence of propylene in the reaction at 350°C is that complete decomposition of ethylene on the catalyst surface predominates any parallel process at temperatures in the range of 350°C. In Chapter 4, the TPR of ethylene on Co/Al_2O_3 showed evidence of decomposition of ethylene beginning at 300°C.

6.3.7 10% Fe/Al_2O_3

Reactions were carried out at 250 and 350°C. Very little ethylene was consumed during the reaction at 350°C. The presence of hydrogen in the final products indicated

that decomposition of ethylene occured to some extent at this temperature. At 250°C, no reaction products were observed.

6.4 DISCUSSION

The hydrogenation of ethylene appears to be predominant in the standard reactions that were studied. It is known that the self-hydrogenation of ethylene readily takes place on most transition metal catalysts. Therefore, ethane observed in the present study would have been produced by self-hydrogenation. For reactions where very small quantities of ethylene were used, ethylene hydrogenation was not observed except in the case of Mo/Al_2O_3 (only at 350°C) and Pt/Al_2O_3. Probably all ethylene remained adsorbed under these conditions.

For the methane-ethylene coupling reaction, Pt/Al_2O_3 shows the best promise amongst the catalysts tested. Trace quantities of propane were produced when a small amount of ethylene was used. Low concentrations of ethylene were used to ensure that some active metal sites were left available to allow for adsorption of methane. The mobility of adsorbate may also be an important factor. On the other hand, the low ethylene concentrations in the reactant gas were reaching the limit of detectability of the gas chromatograph. Trace amounts of propane were only observed at reactions carried out at 250°C, not at higher or lower temperatures. When looking at methane-ethylene coupling in thermodynamic terms, the reaction is practically limited to temperatures below 300°C under the present conditions. The results obtained from the Pt catalyst follow the trend of the thermodynamic equilibrium data. The Pt catalyst showed no changes in behaviour when the catalyst was pretreated in air at 500°C, although there was a significant change observed in the TPR for the same catalyst.

Co/Al_2O_3 was the only catalyst other than Pt/Al_2O_3 to produce higher hydrocarbons using methane and ethylene as reactants under these conditions. The presence of propylene in the final products is not believed to be due to methane-ethylene coupling, but possibly due to butene formation followed by cracking to propylene. The direct formation of propylene from methane and ethylene cannot be expected thermodynamically.

When comparing the results of the TPR experiments with the methane-ethylene coupling reactions, some discrepancies arise. In TPR, decomposition of methane started, in most cases, at temperatures below 200°C as seen in Table 4.1, while in the coupling reaction, methane remained almost unchanged at reaction temperatures up to 350°C. The TPR of ethylene showed that ethylene adsorbed upon contact on all catalysts except Pd, Pt and Ir, where C_2H_4 did not observably adsorb until higher temperatures. Ethylene decomposed at temperatures above 300°C in most cases (Table 4.3). In the methane-ethylene coupling reaction, therefore, ethylene strongly adsorbs on the metal sites and probably no sites are available for methane decomposition. At the same time, the site blocking by ethylene would also prevent the coupling reaction from taking place.

In the case of Pt/Al_2O_3, ethylene did not observably adsorb on the catalyst surface in the TPR experiments until the temperature reached 240°C. Therefore, in the methane-ethylene coupling reactions, ethylene interference would not be too strong at reaction temperatures of approximately 240°C or below. The presence of propane in the final products for the coupling reaction carried out at 250°C suggests that methane was being dissociated on the catalyst surface. Propane was not produced for coupling reactions carried out at 350°C. With higher pressure of ethylene however, the coupling reaction will be difficult even at 250°C because of an increase in the site blocking by ethylene.

Pd/Al_2O_3 and Ir/Al_2O_3 were the other catalysts that showed ethylene adsorption only at higher temperatures in the TPR experiments. Ethylene started adsorbing on the Pd and Ir catalysts at 130 and 110°C respectively. Therefore, the blocking effect may be somewhat weaker than other catalysts except for Pt. The coupling reaction may be possible with less coverage of the sites by ethylene. Unfortunately, further reduction of ethylene could not be made because of the detection limit of the system for propane.

6.5 SUMMARY

The 1% Pt/Al_2O_3 catalyst appears to be the most promising of the catalysts that were studied for methane-ethylene coupling. The quantities of propane produced under the conditions used were small.

Chapter 7

CONCLUSIONS

The interaction of methane and ethylene were investigated on various supported metal catalysts mainly by the temperature programmed reaction (TPR) technique. The isothermal reaction of methane also revealed that the dissociation of methane proceeds quite differently on these catalysts.

The Methane-ethylene coupling reaction was observed only with 1% Pt/Al_2O_3 catalyst. The advantage of the Pt catalyst and the failure of other catalysts were explained by the difference in the interaction of ethylene with the metal sites based on the information obtained from the TPR experiments.

APPENDIX A

Table A.1 Characterization of Catalysts

CATALYST	MASS OF CATALYST (g)	% METAL	QUANTITY OF ADSORBED H_2 (moles)
Ni/Al_2O_3[ab]	0.4573	5	8.052×10^{-6}
Ni/SiO_2[bc]	0.3142	5	2.462×10^{-6}
Ni/SiO_2[c]	0.4357 0.1388	9.6	2.911×10^{-5} 1.050×10^{-5}
Mo/Al_2O_3[b]	0.6588	10-12	2.257×10^{-5}
Co/Al_2O_3[c]	0.5345 0.2146	9.5	1.286×10^{-5} 1.850×10^{-5}
Fe/Al_2O_3[c]	0.3965	10.0	1.262×10^{-6}
Ru/Al_2O_3	0.4361	0.5	3.292×10^{-7}
Pt/Al_2O_3	1.0542	1.0	9.344×10^{-6}
Rh/Al_2O_3	0.4836	0.5	2.058×10^{-6}
Re/Al_2O_3	0.4023	0.5	
Pd/Al_2O_3	0.5225	0.5	3.784×10^{-6}
Ir/Al_2O_3	0.4563	1.0	4.300×10^{-5}

[a] precipitated
[b] calcined
[c] impregnated

APPENDIX B

Methane and ethylene TPR profiles (not shown in Chapter 4)

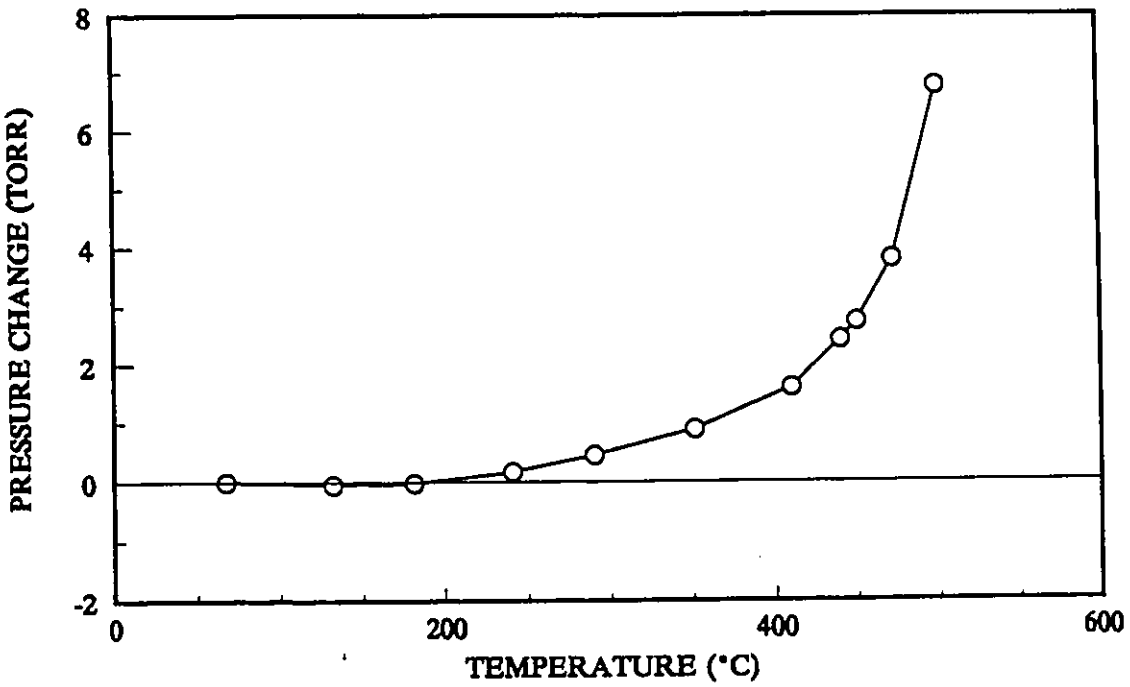

Figure B.1 Methane TPR profile for 5% Ni/Al_2O_3

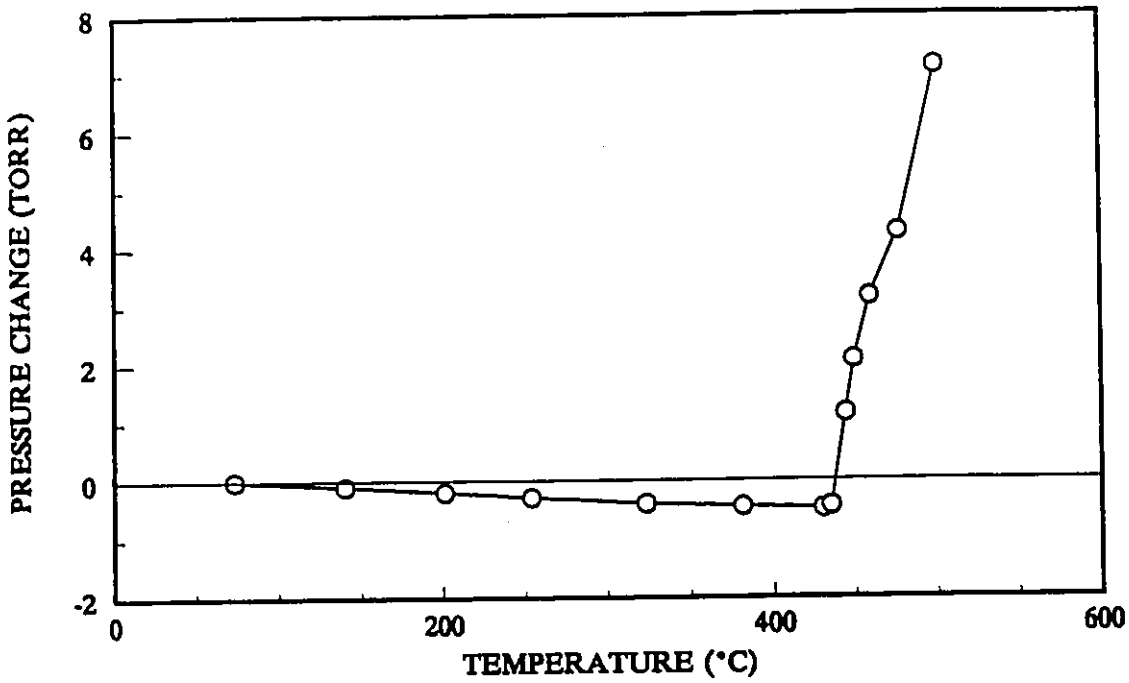

Figure B.2 Methane TPR profile for 5% NiO/Al_2O_3

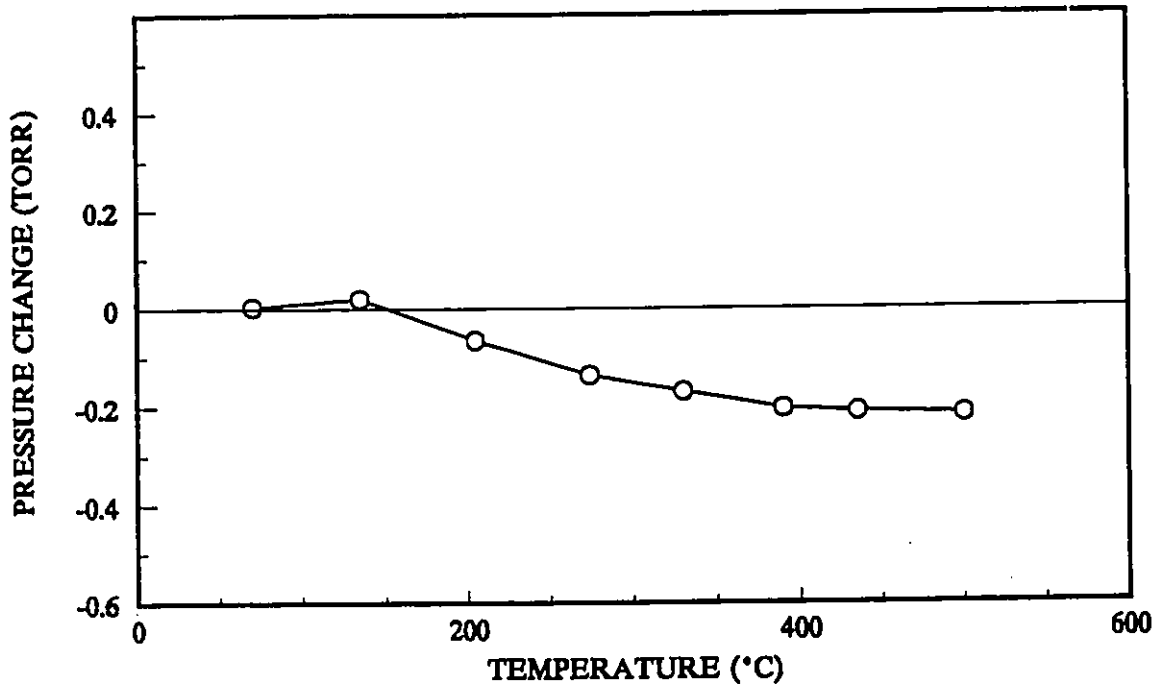

Figure B.3 Methane TPR profile for 9.6% NiO/SiO_2

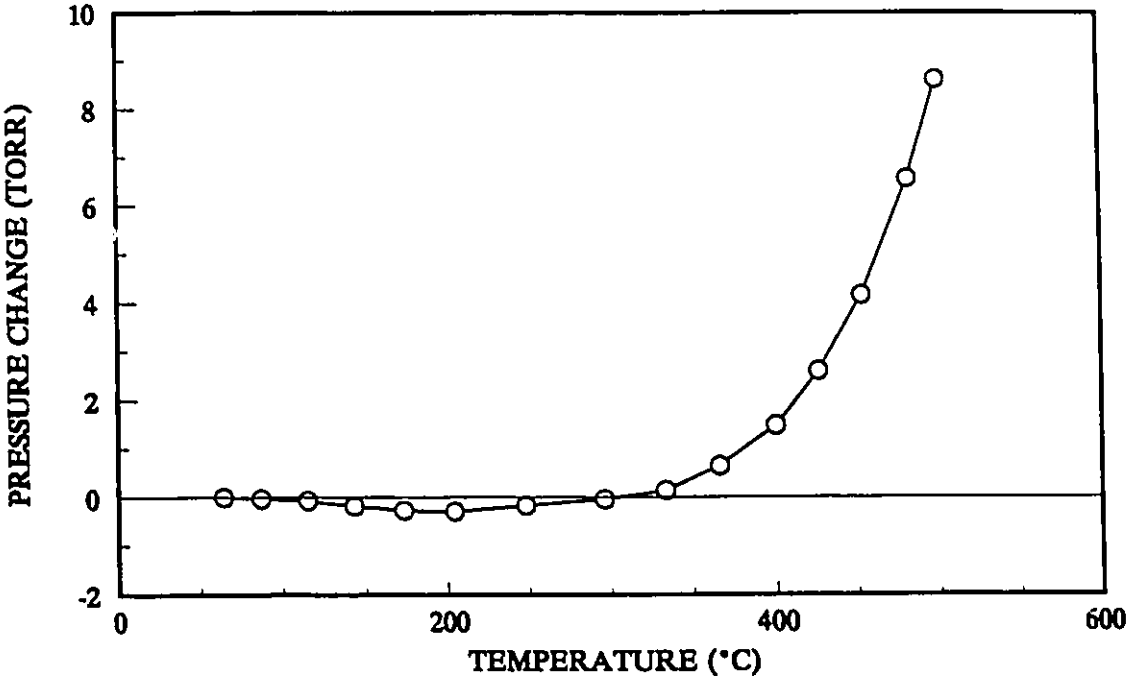

Figure B.4 Methane TPR profile for 0.5% Rh/Al_2O_3

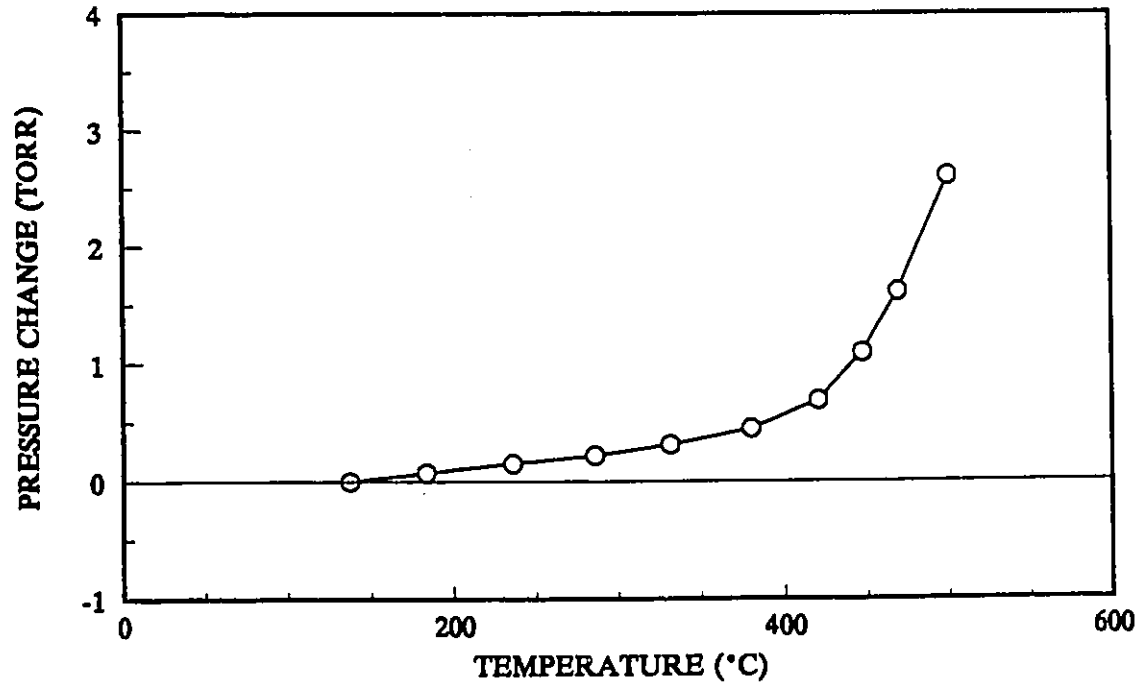

Figure B.5 Methane TPR profile for 0.5% Pd/Al_2O_3

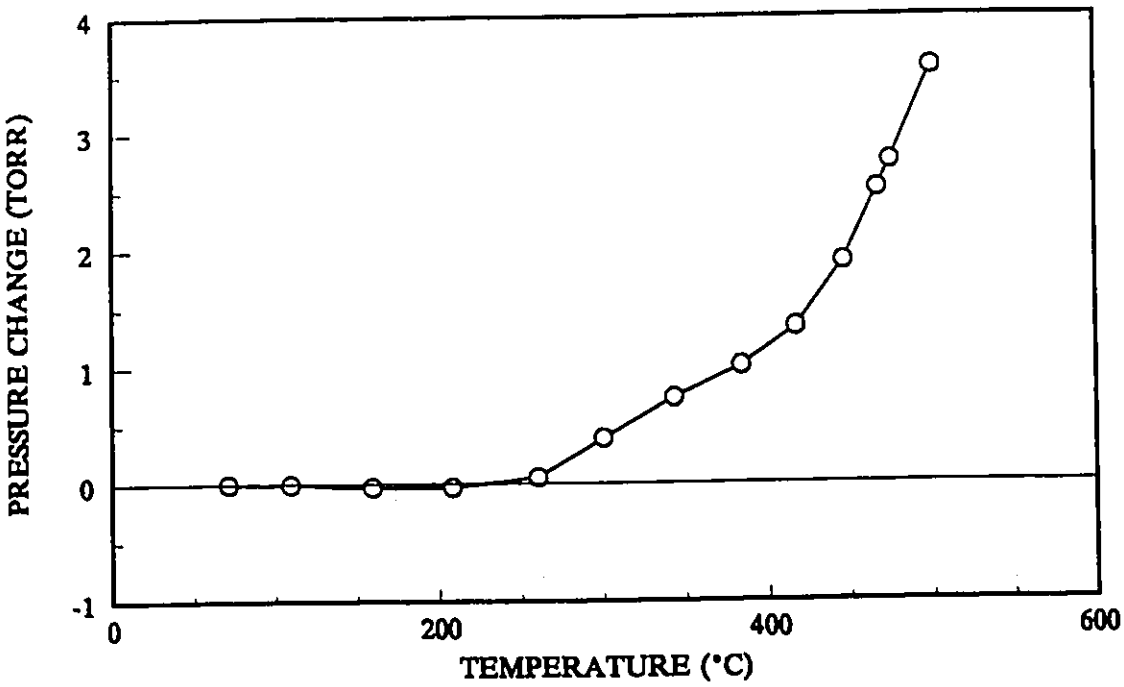

Figure B.6 Methane TPR profile for 1% Ir/Al_2O_3

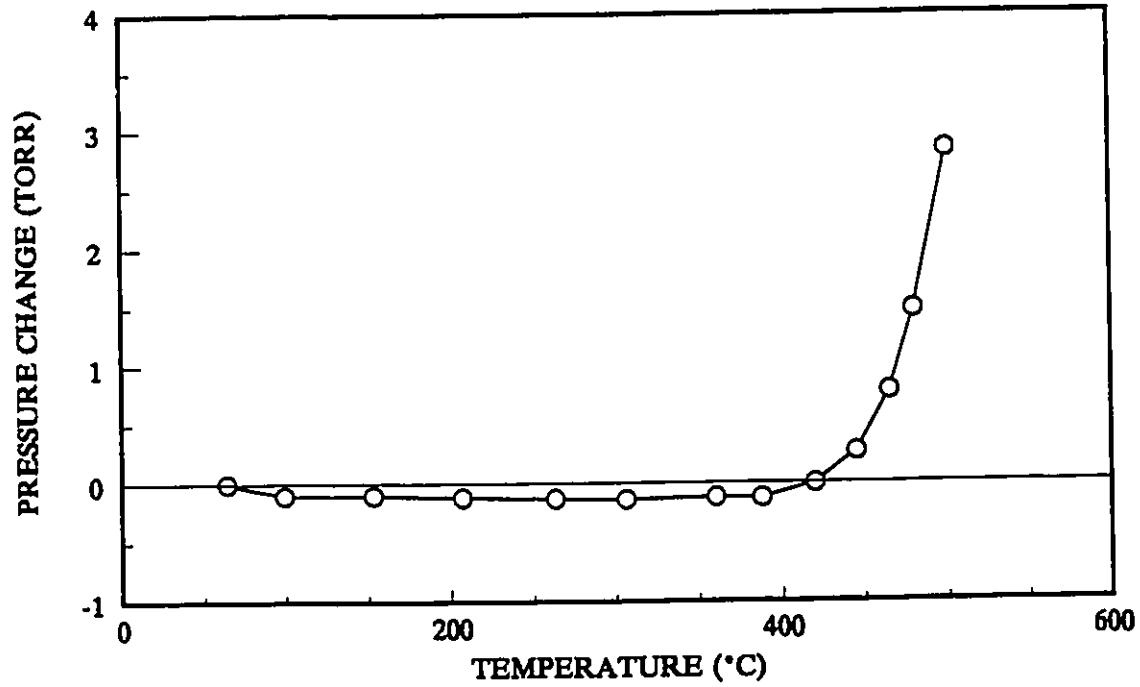

Figure B.7 Methane TPR profile for 0.5% Re/Al_2O_3

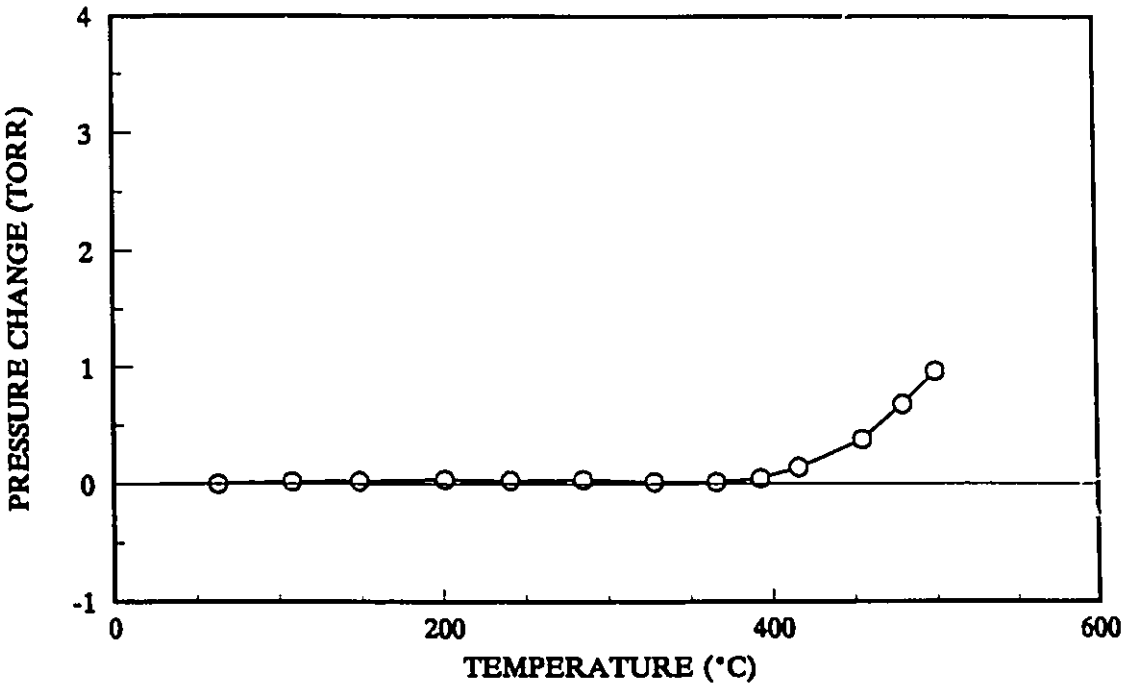

Figure B.8 Methane-Ethylene TPR profile for 0.5% Re/Al_2O_3

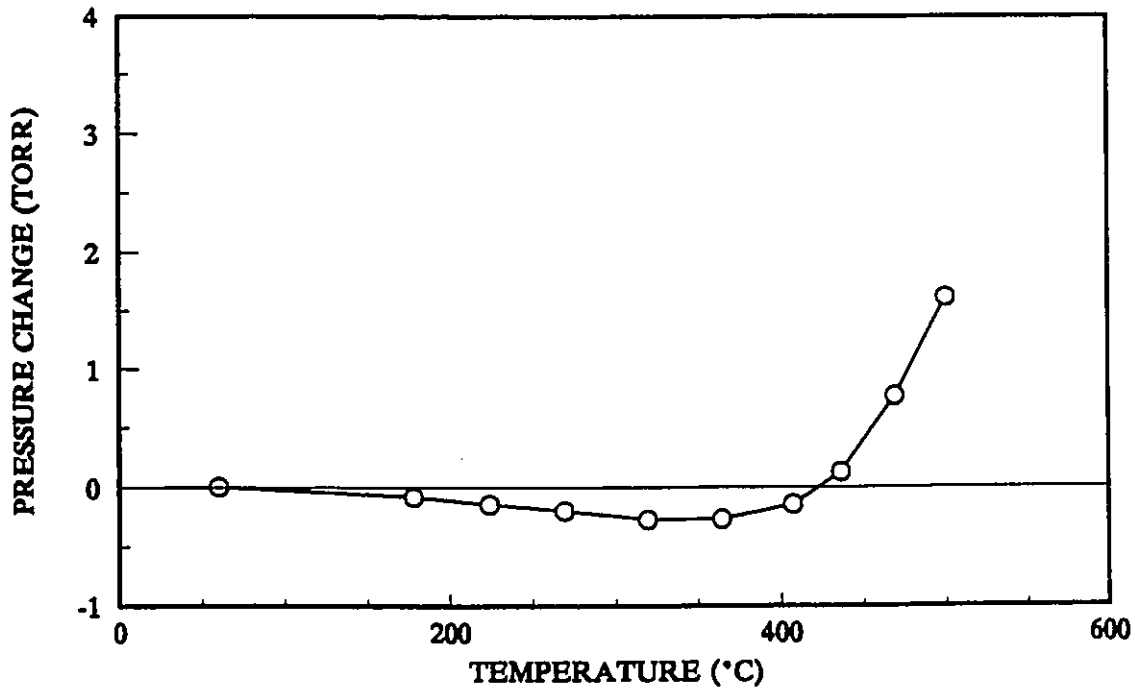

Figure B.9 Methane TPR profile for 11% Mo/Al_2O_3

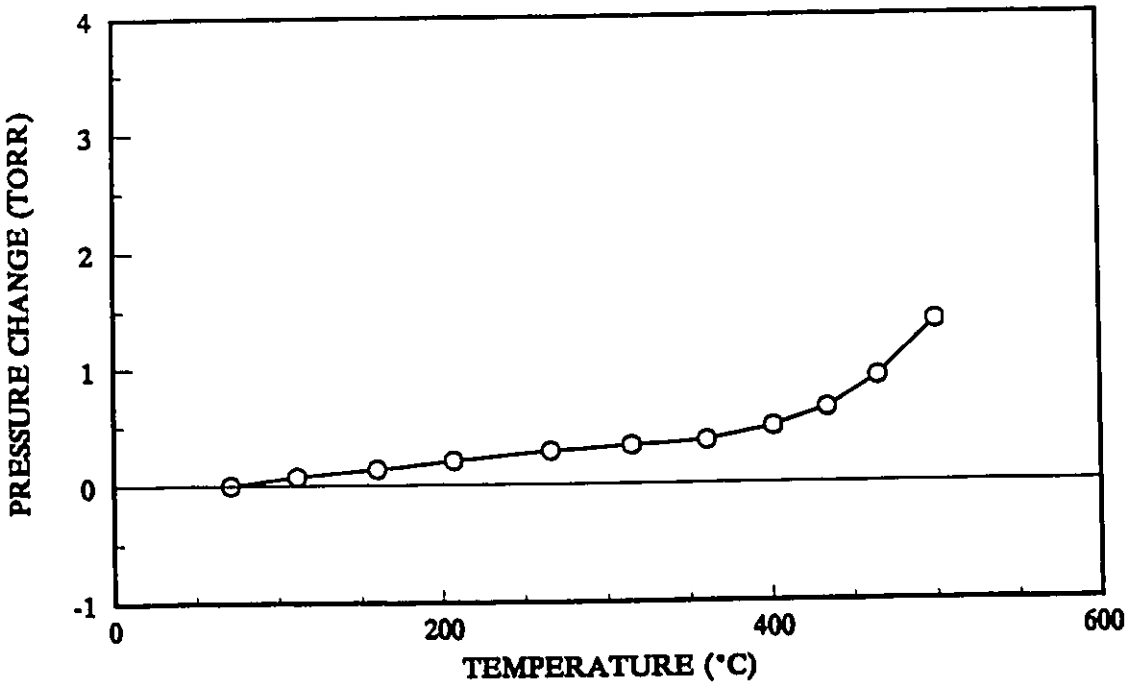

Figure B.10 Methane TPR profile for 10% Fe/Al_2O_3

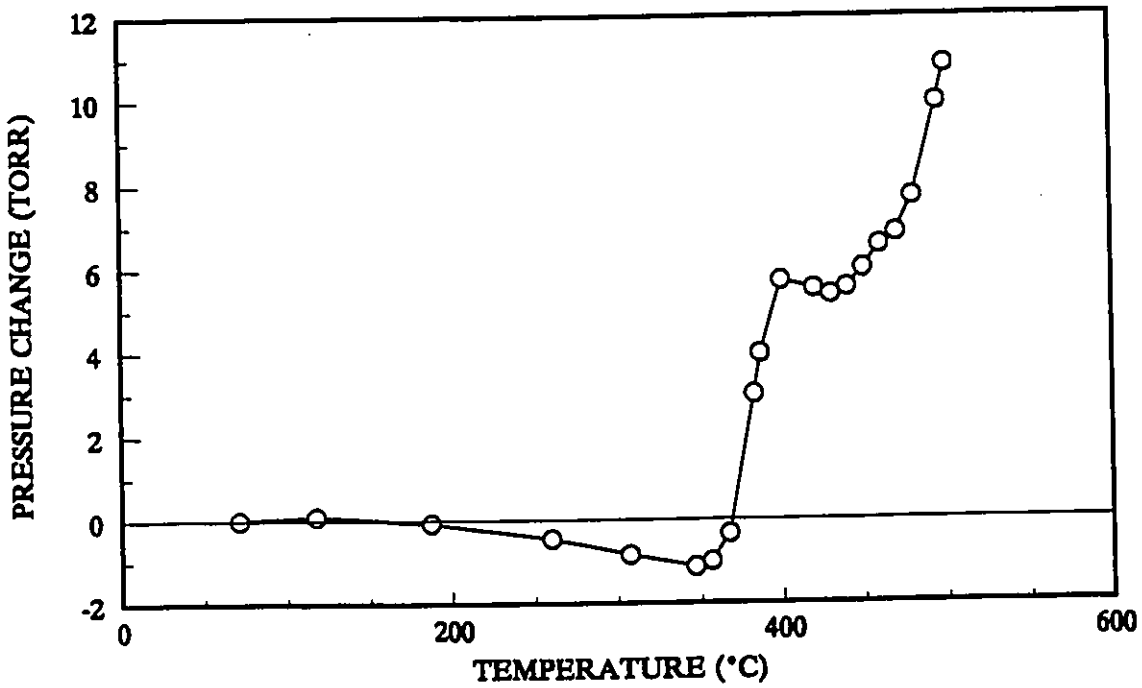

Figure B.11 Ethylene TPR profile for 5% NiO/Al_2O_3

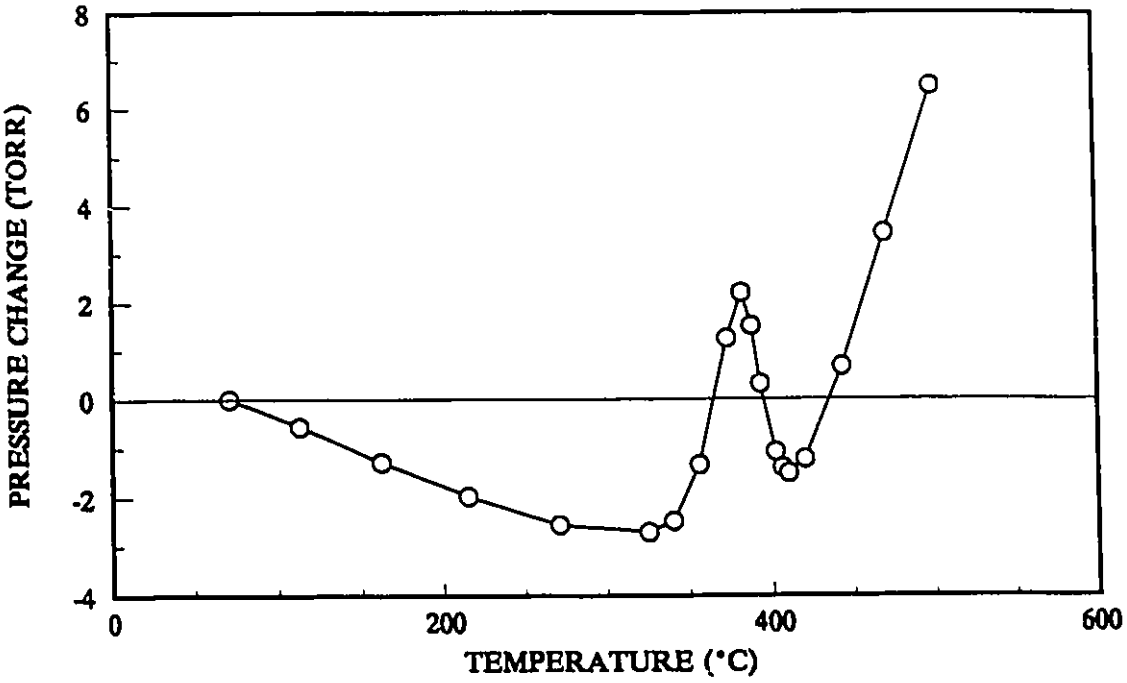

Figure B.12 Ethylene TPR profile for 9.6% NiO/SiO_2

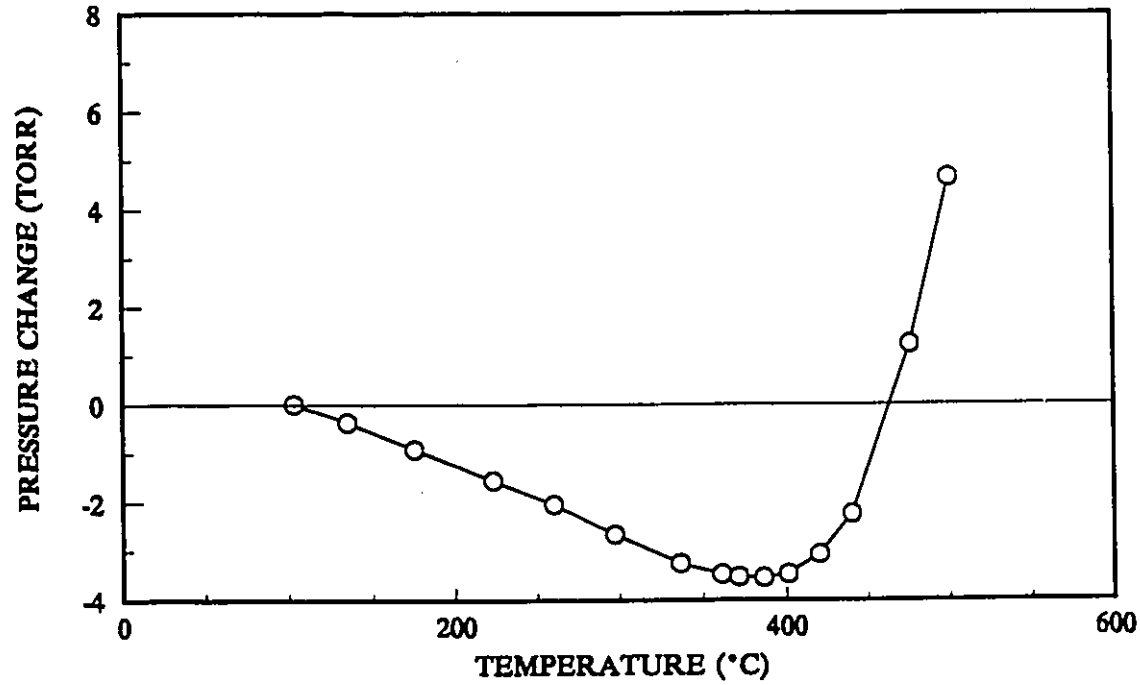

Figure B.13 Ethylene TPR profile for 1% Pt/Al_2O_3 pretreated with air

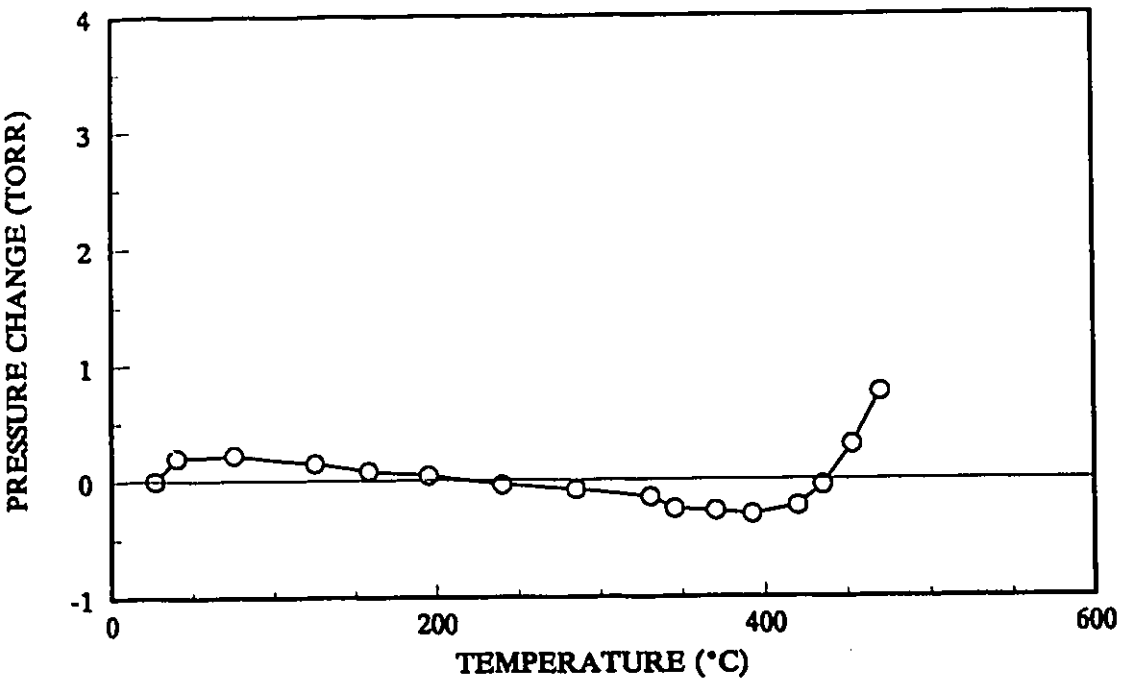

Figure B.14 Ethylene TPR profile for 1% Pt/Al_2O_3

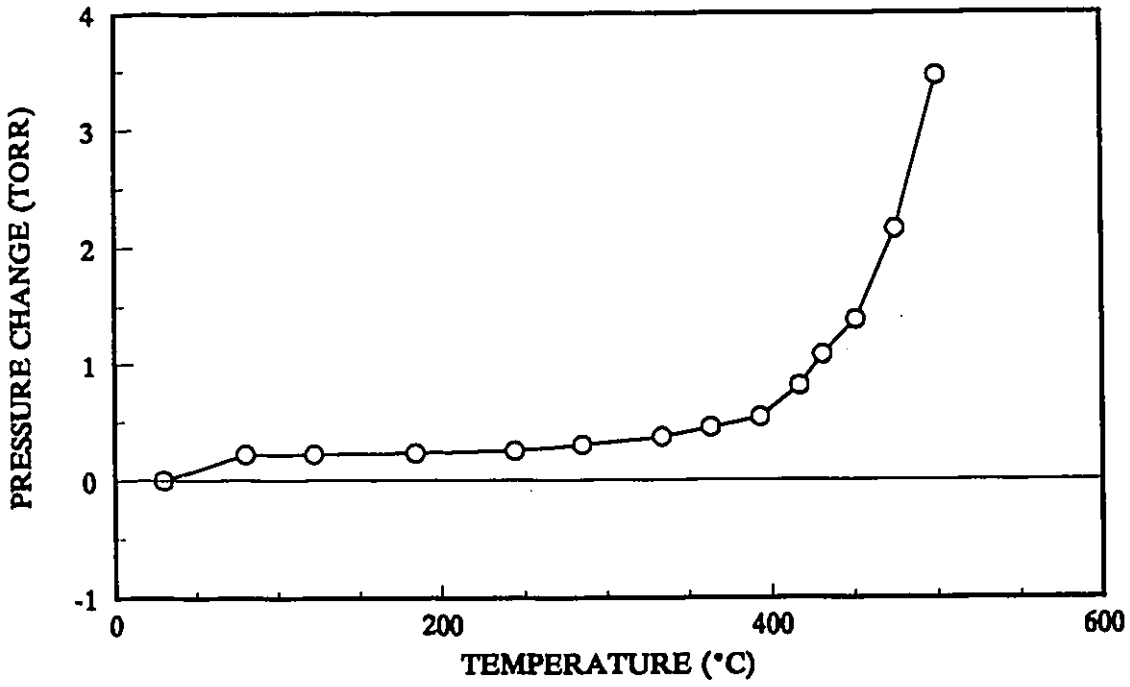

Figure B.15 Methane TPR profile for 1% Pt/Al_2O_3

APPENDIX C

Chromatographic Data from the Analysis of Final Products of the Coupling Reactions

Figure C.1 Calibration Chromatogram from the FID

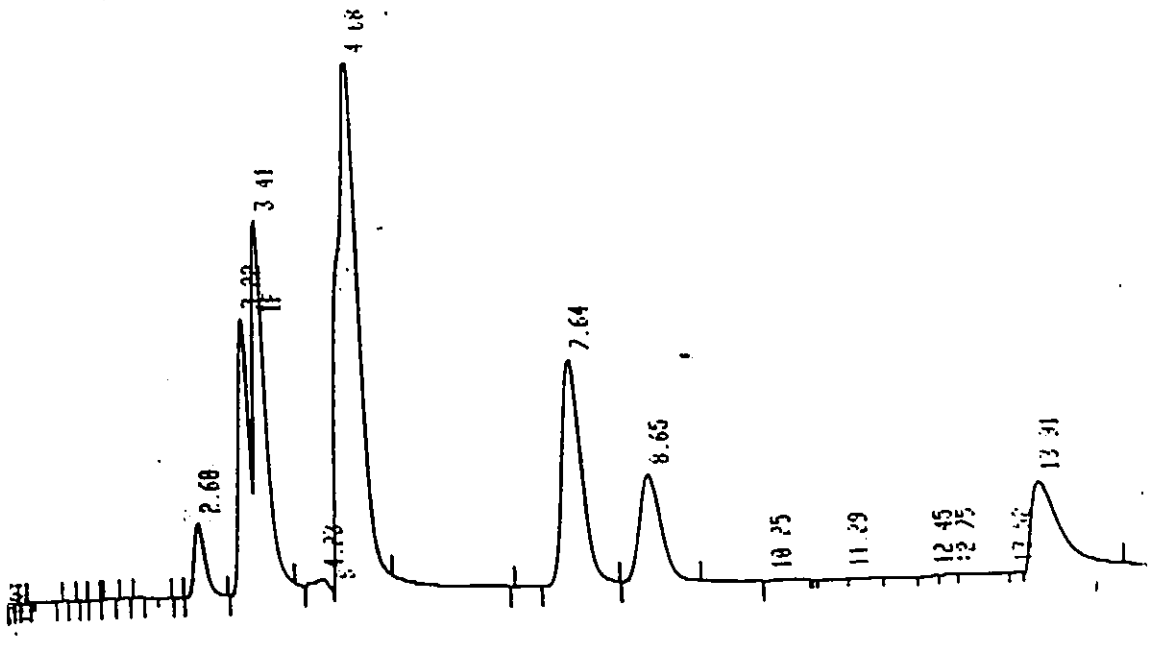

RETENTION TIME (min)	HYDROCARBON
2.60	CH_4
3.22	C_2H_6
3.41	C_2H_4
4.68	C_3
7.64	iso-C_4H_{10}
8.65	n-C_4H_{10}
13.91	1-C_4H_8

Figure C.2 Calibration Chromatogram from the TCD

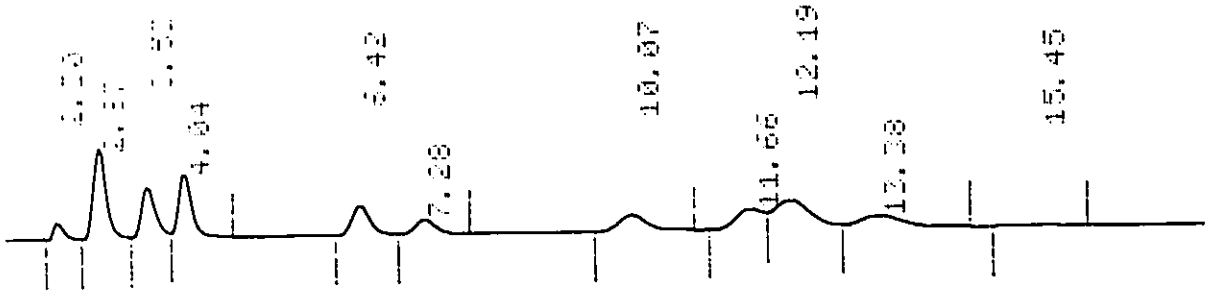

RETENTION TIME (min)	HYDROCARBON
2.30	CH_4
2.87	C_2
3.53	C_2H_2
4.04	C_3H_8
6.42	C_3H_6
7.28	n-C_4H_{10}
10.07	1-C_4H_8
11.66	iso-C_4H_{10}
12.19	trans C_4H_8
13.38	cis C_4H_8
15.45	n-C_5H_{12}

REFERENCES

1. Amenomiya, Y., Birss, V.I., Goledzinowski, M., Galuszka, J., Sanger, A.R., Catal. Rev. -Sci. Eng. 32, 163 (1990); Lee, J.S., Oyama, S.T., Catal. Rev. -Sci. Eng. 30, 24 (1988); Anderson, J.R., Appl. Catal. 47, 177 (1989).

2. Keller, G.E., Bhasin, M.M., J. Catal. 73, 9 (1982).

3. Siskin,A., J. Am. Chem. Soc. 98, 5413 (1976).

4. Sommer, J., Muller, M., Laali, K., Nov. J. Chim. 1, 3 (1982).

5. Olah, G.A., Felberg, J.D., Lammertsma, K., J. Am. Chem. Soc. 105, 6529 (1983).

6. Scurrell, M.S., Appl. Catal. 34, 109 (1987).

7. Ovalles, C., Leon, V., Reyes, S., Rosa, F., J. Catal. 129, 368 (1991).

8. Loffler, D., Maier, W.F., Andrade, J.G., Thies, I., von Rague Schleyer, P., J. Chem. Soc., Chem. Commun., 1177 (1984).

9. Anderson, A.B., Maloney, J.J., J. Phys. Chem. 92, 809 (1988).

10. Gaidai, N.A., Babernich, L., Guczi, L., Kinet. Katal. 15, 974 (1974).

11. Kuijpers, E.G.M., Jansen, J.W., Van Dillen, A.J., Geus, J.W., J. Catal. 72, 75 (1981).

12. Hamza, A.V., Madix, R.J. Surf. Sci. 179, 25 (1987).

13. Szuromi, P.D., Engstron, J.R., Weinberg, W.H., J. Phys. Chem. 89, 2497 (1985).

14. Stewart, C.N., Ehrlich, G., J. Chem. Phys. 62, 4672 (1975).

15. Kuijpers, E.G.M., Breedik, A.K., Van Der Wal, W.J.J., Geus, J.W., J. Catal. 72, 210 (1981).

16. Kuijpers, E.G.M., Breedik, A.K., Van Der Wal, W.J.J., Geus, J.W., J. Catal. 81, 429 (1983).

17. Kuijpers, E.G.M., Kock, A.J.H.M., Wermer, G.J., Geus, J.W., J. Catal.88, 1 (1984).

18. Erkelens, J., Wosten, W.J., J. Catal. 54, 143 (1978).

19. Shuit, G.C.A., van Reijen, L.L., Advan. Catal. 10, 242 (1958).

20. Slinken, A.A., Kucherov, A.V., Rubinshtein, A.M., Kinet. Catal. (USSR) 9(2), 415 (1978).

21. Bartholomew, C.H., Pannell, R.B., J. Catal. 65, 390 (1980).

22. Brooks, C.S., Christopher, G.L.M., J. Catal., 10, 211, (1968); Taylor, W.F., Sinfelt, J.H., J. Amer. Chem. Soc. 86, 2996 (1964).

23. Selwood, P.W., J. Catal. 42, 148 (1976).

24. Pannell, R.B., Chung, K.S., Bartholomer, C.H., J. Catal. 46, 340 (1977).

25. Bartholomew, C.H., Farrauto, R.J., J. Catal. 45, 41 (1976).

26. Kuijpers, E.G.M., Nieuwesteeg, M.W.C.M.A., Wermer, G.J., Geus, J.W., J. Catal. 112, 107 (1988).

27. Yates, D.J.C., Taylor, W.F., Sinfelt, J.H., J. Am. Chem. Soc. 86, 2996 (1964).

28. Bartholomew, C.H., Boudart, M., J. Catal. 25, 173 (1972).

29. Remey, H., "Treatise on Inorganic Chemistry", Vol. II, pp. 310 Elsevier, Amsterdam (1956).

30. Hill, F.N., Selwood, P.W., J. Am. Chem. Soc. 71, 2522 (1949).

31. Galuszka, J., Sawicki, J.A., Ottawa Area Catalysis Discussion Meeting, CANMET Energy Research Laboratories, Nov. 2, 1990.

32. Johnson, K.H., Balazs, A.C., Kolari, H.J., Surface Sci. 72, 733 (1978); Horsley, J.A., J. Am. Chem. Soc. 101, 2870 (1979); Haberlandt, H. Ritschl, F., J. Phys. Chem. 87, 3244 (1983).

33. Rameswaran, M., Bartholomew, C.H., J. Catal. 117, 218 (1989).

34. Steininger, H., Ibach, H., Lehwald, S., Surf. Sci. 117, 685 (1982).

35. Hatzikos, G.H., Masel, R.I., Surf. Sci. 185, 479 (1987).

36. Beebe, T.P., Jr., Yates, J.T., J., J. Phys. Chem. 91, 254 (1987).

37. Wang, P.-K., Slichter, C.P., Sinfelt, J.H., J. Phys. Chem. 89, 3606 (1985).

38. Koel, B.E., Bent, B. E., Somorjai, G.A., Surf. Sci. 146, 211 (1984).

39. Kesmodel, L.L., Dubois, L.H., Somorjai, G.A., J. Chem. Phys. 70, 2180 (1979).

40. Kesmodel, L.L., Dubois, L.H., Somorjai, G.A., Chem. Phys. Lett. 56, 267 (1978).

41. Koestner, R.J., Van Hove, M.A., Somorjai, G.A., Surf. Sci. 121, 321 (1982).

42. Barteau, M.A., Broughton, J.Q., Menzel, D., Appl. Surf. Sci. 19, 92 (1984).

43. Kesmodel, L.L., Gates, J.A., Surf. Sci. 111, 1747 (1981).

44. Beebe, T.P., Jr., Albert, M.R., Yates, J.T., Jr., J. Catal. 96, 1 (1985).

45. Kang, D.B., Anderson, A.B., Surf. Sci. 155, 639 (1985).

46. Lapinski, M.P., Ekerdt, J.G., J. Phys. Chem. 92, 1708 (1988).

47. McKee, D.W., J. Phys. Chem. 84, 1109 (1962).

48. Stuve, E.M., Madix, R.J., J. Phys. Chem. 89, 105 (1985).

49. Bent, B.E., Ph.D. Thesis, University of California, Berkeley (1986).

50. Lehwald, S., Ibach, H., Surf. Sci. 89, 425 (1979).

51. Stroscio, J.A., Bare, S.P., Ho, W., Surf. Sci. 148, 499 (1984).

52. Zaera, F., Hall, R.B., J. Phys. Chem. 91, 4318 (1987).

53. Rickard J.M., Genovese, L., Moata, A., Nitsche, S., J. Catal. 121,141 (1990).

54. Olah, G.A., Eur. Pat. Appl. EP 73,673 09 Mar 1983, U.S. Appl. 298,486 01 Sep 1981.